remote sensing

MDPI

Article

UAV LiDAR Survey for Archaeological Documentation in Chiapas, Mexico

Whittaker Schroder [1,*], Timothy Murtha [1], Charles Golden [2], Andrew K. Scherer [3], Eben N. Broadbent [1,4], Angélica M. Almeyda Zambrano [1], Kelsey Herndon [5] and Robert Griffin [5]

1 Center for Latin American Studies, Florida Institute for Built Environment Resilience, The University of Florida, 720 SW 2nd Ave, Gainesville, FL 326011, USA; tmurtha@ufl.edu (T.M.); eben@ufl.edu (E.N.B.); aalmeyda@ufl.edu (A.M.A.Z.)
2 Department of Anthropology, Brandeis University, 415 South St., Waltham, MA 02453, USA; cgolden@brandeis.edu
3 Department of Anthropology, Brown University, Providence, RI 02912, USA; andrew_scherer@brown.edu
4 School of Forest, Fisheries, and Geomatics Sciences, University of Florida, Gainesville, FL 326011, USA
5 Department of Atmospheric and Earth Science, University of Alabama in Huntsville, 320 Sparkman Drive, Huntsville, AL 35899, USA; keh0023@uah.edu (K.H.); reg0005@uah.edu (R.G.)
* Correspondence: wschroder@ufl.edu

Abstract: Airborne laser scanning has proven useful for rapid and extensive documentation of historic cultural landscapes after years of applications mapping natural landscapes and the built environment. The recent integration of unoccupied aerial vehicles (UAVs) with LiDAR systems is potentially transformative and offers complementary data for mapping targeted areas with high precision and systematic study of coupled natural and human systems. We report the results of data capture, analysis, and processing of UAV LiDAR data collected in the Maya Lowlands of Chiapas, Mexico in 2019 for a comparative landscape study. Six areas of archaeological settlement and long-term land-use reflecting a diversity of environments, land cover, and archaeological features were studied. These missions were characterized by areas that were variably forested, rugged, or flat, and included pre-Hispanic settlements and agrarian landscapes. Our study confirms that UAV LiDAR systems have great potential for broader application in high-precision archaeological mapping applications. We also conclude that these studies offer an important opportunity for multi-disciplinary collaboration. UAV LiDAR offers high-precision information that is not only useful for mapping archaeological features, but also provides critical information about long-term land use and landscape change in the context of archaeological resources.

Keywords: LiDAR; UAV; mapping; archaeology; Mesoamerica

Citation: Schroder, W.; Murtha, T.; Golden, C.; Scherer, A.K.; Broadbent, E.N.; Almeyda Zambrano, A.M.; Herndon, K.; Griffin, R. UAV LiDAR Survey for Archaeological Documentation in Chiapas, Mexico. *Remote Sens.* **2021**, *13*, 4731. https://doi.org/10.3390/rs13234731

Academic Editor: Timo Balz

Received: 27 October 2021
Accepted: 17 November 2021
Published: 23 November 2021

1. Introduction

Airborne LiDAR has transformed archaeological mapping and prospection, especially in densely forested neotropical regions [1–9]. Increasingly, these data are being acquired to produce rapid maps of land surfaces, archaeological features, and archaeological landscapes [10–12]. Exemplary archaeological applications have been tightly coupled to multi-disciplinary studies of forests and natural systems [13–18]. These studies offer unparalleled information about coupled natural human systems and regional landscapes. As LiDAR systems evolve, terrestrial and UAV applications are increasingly subject to experimentation. As currently configured, such smaller-scale systems do not offer broad regional inventories like occupied airborne efforts, but they offer potentially new opportunities for collaboration and precision data about landscapes that are not always accessible via occupied airborne systems. UAV LiDAR is an emerging innovative tool for archaeology, especially archaeological research focused on long-term studies of coupled natural and human systems. This tool is potentially transformative, especially when complemented by occupied airborne LiDAR, UAV photogrammetry, and terrestrial mapping technologies.

The use of unoccupied aerial vehicles (UAVs), or "drones," for mapping has increased recently in several fields, including in ecology, archaeology, and industry, due to improvements in battery efficiency, vehicle portability, and diminishing costs [19–26]. Most recent UAV applications in archaeology largely employ principles of low altitude aerial photography and photogrammetry through Structure from Motion (SfM) algorithms to produce 3D models and maps, with additional studies incorporating thermal and multispectral sensors [27–39]. However, the increasing affordability of lighter weight laser scanning sensors has led to the proliferation of archaeological studies employing UAV-based LiDAR systems. Compared to photogrammetry, LiDAR systems improve terrain mapping in areas of high vegetation cover, alongside the documentation and extraction of above-ground features, including modern structures, archaeological features, and additional layers of canopy [40–47]. While UAV LiDAR applications are increasingly common for studying natural systems and modern infrastructure, we have only recently begun to fully explore their application in archaeology.

Archaeological applications of UAV LiDAR mapping are especially promising for projects that require targeted mapping and/or seasonal or yearly mapping in place of larger-scale aerial surveys that remain cost-prohibitive. The use of UAV LiDAR, particularly in forested tropical environments, is likely to increase, alongside the broader adoption of airborne LiDAR over the past decade as a fundamental part of the archaeologists' toolkit in such regions [48–55]. UAV LiDAR also presents several benefits and challenges over occupied airborne LiDAR, requiring background knowledge of the specific sites targeted for smaller-scale documentation. As the UAV typically follows the natural contours of the landscape rather than flying at a fixed altitude, a fine-grained understanding of the local landscape is necessary to improve data collection. For the most part, due to the limited horizontal coverage of UAVs (1–4 km^2/day) in contrast to occupied airborne systems (>100 km^2/day), drones are less useful for site prospection and better for defining site limits or rapid documentation of targeted areas where ancient settlement has previously been identified. Finally, because drones are piloted from the ground within or adjacent to mission areas, local permissions from modern community authorities and members are of even greater importance in this context, although ideally, local communities and other stakeholders should also be consulted when planning larger-scale occupied airborne missions [56,57].

In this study, we report the results of six UAV LiDAR missions flown in the Maya Lowlands of Chiapas, Mexico in June of 2019 (Figure 1). These six missions were conducted in areas over and around known archaeological sites, documented through pedestrian survey and reconnaissance since 2011 by members of the Proyecto Arqueológico Busiljá–Chocoljá (PABC) and the Proyecto Arqueológico Bajo Lacantún (PABL) working in collaboration with local communities and with permission from the Instituto Nacional de Antropología e Historia (INAH) of Mexico. Locations were selected because they represent a broad sample of archaeological contexts, including large urban centers, smaller rural communities, and relict agricultural fields previously documented in the Usumacinta Region [58]. Importantly, samples were also selected to represent variations in modern land use and physical geography, which we further demonstrate with a land cover classification of the study area. We present several digital elevation or terrain models (DEMs) interpolated from ground classified point returns, demonstrating the success of UAV LiDAR collection in archaeological contexts and the potential for further analyses that build off high-resolution topographic data.

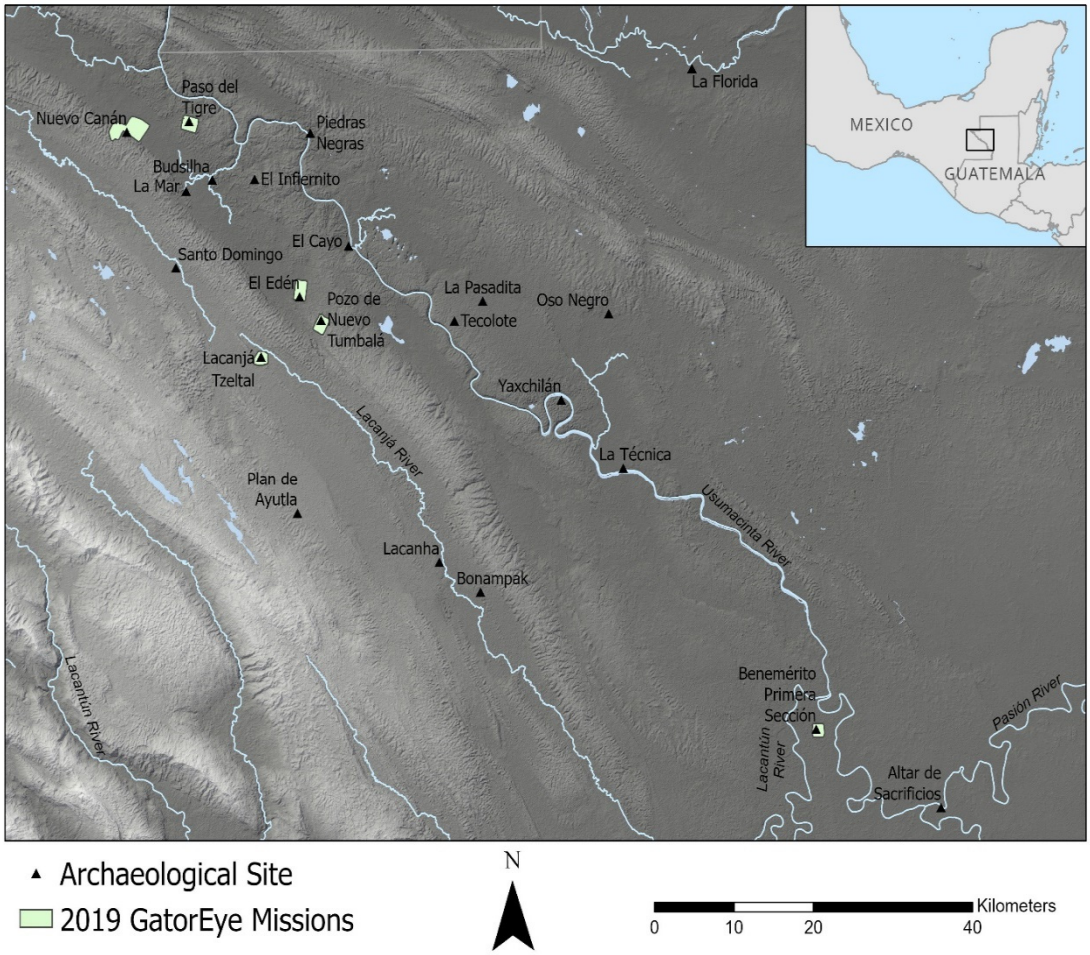

Figure 1. Map of the study area showing the location of archaeological sites and 2019 GatorEye missions.

2. Materials and Methods

This study builds on our pilot UAV LiDAR studies in the Upper Usumacinta River region of the Western Maya Lowlands [44] and is part of a decade-long field-based project studying the archaeological landscapes of the Usumacinta region [59,60]. The Upper Usumacinta River marks the modern border between Mexico and Guatemala for much of its course between the junction with the Pasión River to Boca del Cerro, Tabasco downstream from the archaeological site of Piedras Negras, Guatemala [61–63]. Several archaeological projects have investigated the Mexican and Guatemalan sides of the Usumacinta River since 2003 [64,65]. Our survey efforts were only possible because of this long tradition of research conducted in the region and collaboration with local stakeholders. Our first missions were conducted in Guatemala and Mexico [44], but the missions discussed here were conducted only in Mexico because of the variation in vegetation, landform, land use, and accessibility. The complexity of this variation offered a variety of contexts to investigate how the location, sample size, and processing influences the quality of data collected.

The Usumacinta region is characterized by a complex natural and cultural landscape of ridges and valleys with diverse modern land-use regimes, including recently cleared areas for agriculture and cattle grazing, zones of secondary growth, and protected areas with high canopy. The karst landscape also presents finer-grained variations in the physical geography, including exposed limestone ridges, sinkholes, and cliffs. Archaeological remains in the region are diverse, with large Classic period (250–900 CE) royal centers such as Piedras Negras, Lacanjá Tzeltal, and La Mar, as well as rural farming communities, fortified villages, and relict agrarian landscapes (see Figure 1, sites and samples). This complexity provides a suitable case study to test the efficacy of UAV LiDAR survey for archaeological applications. We report here the results of 6 missions flown in Chiapas,

Mexico: Paso del Tigre, Benemérito de las Américas Primera Sección, Edén-Jovero, Nuevo Canán, Lacanjá Tzeltal, and El Pozo de Nuevo Tumbalá.

To better document and quantify the diversity of land uses and land cover in the region, we developed a basic classification coverage, relying on 2019 imagery and Google Earth Engine. In the current study, this land cover classification did not inform LiDAR point processing, as we opted to apply the same processing workflow to each mission. Instead, the land cover classification demonstrates the success of UAV LiDAR mapping in diverse environments. At the same time, an understanding of the modern land use of the region alongside the physical geography can identify areas for improvement in planning future missions. The 2019 landcover classification was created using Sentinel-2 imagery processed in Google Earth Engine (GEE) [66] (Figure 2). The Sentinel-2 Multispectral Instrument (MSI) level 2A (L2A) product representing surface reflectance was filtered by date to scenes from 2019 and by location to scenes covering our study area, resulting in 441 individual images [67]. The S2 cloud probability dataset provided by GEE and generated using the Sentinel Hub sentinel-2-cloud-detector library was joined to the Sentinel-2 MSI L2A image collection. Individual S2 scenes were then masked using a cloud probability threshold of 10. The cloud masked image collection was composited using the median function, resulting in a cloud-free 2019 Sentinel-2 image composite. Next, polygons for each land cover classification category (forest, grassland/cropland, built/bare, and water) were created based on visual inspection of the Sentinel-2 imagery. Points generated from these polygons were split into training (80%) and testing (20%) datasets. A random forest classifier (with n = 100 trees) was applied to the 2019 S2 image composite using bands 1-8A and resulting in a four-class land cover map. The accuracy of the map was evaluated using the testing dataset; overall accuracy was 0.99, with the most frequent misclassification from the grass/crop class being classified as forest [68]. See Table 1 for a confusion matrix and Table 2 for the land cover area for each sample site. The confusion matrix is used to compare the number of pixels predicted to represent a land cover category with the actual land cover type, identified visually in the testing dataset. For example, all pixels representing water were correctly classified, while 350 forest pixels were incorrectly classified as grass/crop.

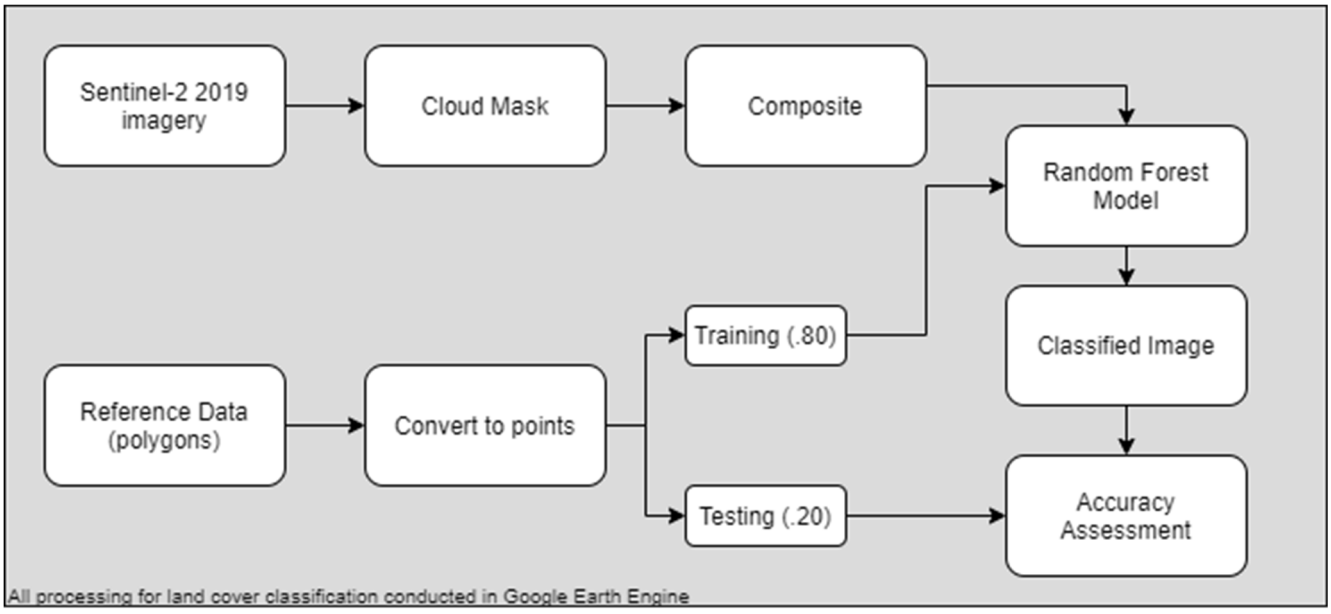

Figure 2. Flowchart showing the workflow used for the land cover classification in Google Earth Engine.

Table 1. Confusion matrix for land cover classification testing dataset.

		Actual				
		Forest	**Grass/Crop**	**Built/Bare**	**Water**	**Total**
Predicted	forest	35,141	95	0	0	35,236
	grass/crop	350	13,360	0	0	13,710
	built/bare	0	32	246	0	278
	water	0	0	0	1590	1590
	Total	35,491	13,487	246	1590	50,814

Table 2. Landcover in square kilometers for each sample discussed here.

Site	Forest: Grassland Ratio	Forest Cover	Crop and Grassland	Urbanized Area	Water	Total
Paso del Tigre	0.722	1.36	1.88	0	0	3.24
Benemérito Primera Sección	0.0271	0.0590	2.18	0.000589	0	2.24
Edén-Jovero	1.01	1.71	1.70	0.000981	0	3.41
Nuevo Canán	0.660	3.35	5.07	0.0766	0.0209	8.52
Lacanjá Tzeltal	0.766	1.04	1.36	0.000196	0.000981	2.40
El Pozo	6.49	2.54	0.392	0	0	2.93

Each sample area land cover is visible in Table 2. Additionally, a ratio of forest to grassland was calculated for each of the sample sites to create a simple metric to compare each sample's vegetation cover. Most of the sites exhibit more grassland than forested area; however, sites such as Benemérito Primera Sección and El Pozo exhibit extreme variation in the land cover ratios.

The data discussed here were collected using the University of Florida's GatorEye Unoccupied Flying Laboratory (www.gatoreye.org, accessed on 18 November 2021), a custom-designed complete UAV remote sensing platform. Our 2019 flights used a custom Scout-32 system from Phoenix LiDAR (https://www.phoenixlidar.com/scout-32, accessed on 18 November 2021). Our two pilot studies also used Phoenix systems, including a previous custom Scout-16 GatorEye system in the Usumacinta River region in 2018 [44,69]. Our 2017 pilot study used a miniRANGER sensor (http://www.phoenixlidar.com/miniranger, accessed on 18 November 2021) and was focused on the monumental center of Piedras Negras, Guatemala. Smaller sites in Mexico, Budsilha and El Infiernito in Chiapas, were the focus of our pilot studies in 2018. These data were acquired using the original GatorEye custom Scout-16 (http://www.phoenixlidar.com/scout-16, accessed on 18 November 2021). Field observations were collected during a two-week period as part of a broader study of lowland Maya settlement and land use, relying on existing occupied airborne LiDAR surveys from 2013 and ongoing LiDAR data acquisition [12,58,70].

Laser point positions were accurately solved in UTM coordinates using observations associated with the positional coordinates of the airborne sensor and the angular orientation of the aircraft. Positions were estimated using integrated kinematic processing of data collected from an onboard global navigation satellite system (GNSS) unit and an inertial measurement unit (IMU) to determine angular orientation. Sensors were geolocated to $\pm$2.5 cm using observations from a dual-frequency GNSS unit, with angular orientation obtained using a high-resolution tactical grade IMU (STIM 300) and integrated post-processed kinematic algorithms relative to a GNSS base station using NovAtel InertialExplorer software. The drone was flown at approximately 80 m above ground level, at a 10 m/s speed, with equally spaced transects about 80 m apart, employing a crosshatch flight pattern to maximize point density and coverage along inclined surfaces.

3. Results

We conducted six missions in Chiapas, Mexico during the 2019 season (Figure 1) [71]. Ground points were classified with semi-automated packages: the set of tools available in ESRI ArcGIS Pro 2.8.3 and LAStools (http://lastools.org, accessed on 18 November 2021), which can be run as standalone executables or through ArcGIS Pro or open-source software (e.g., QGIS 3.16.6). Open-source tools, including the lidR package in R (https://cran.r-project.org/web/packages/lidR/index.html, accessed on 18 November 2021), also produced quality results; however, in this article, we focus on straightforward processing using ArcGIS Pro's proprietary algorithm [72] to effectively compare the results of field samples, rather than focus on variations in processing results, and to demonstrate ease of use.

In ArcGIS Pro, we first created an LAS dataset (.lasd) followed by two iterations of the Classify LAS Ground tool, first with the ground detection method set to standard, followed by an aggressive classification reusing existing ground points for nearly all missions due to the rugged topography and variable vegetation. In the Benemérito Primera Sección mission, a single iteration of the standard classification sufficed due to the surrounding landscape of a relatively flat upland region adjacent to the floodplain, dominated by grassland with patches of secondary growth. The LAS Dataset to Raster tool was then used with default settings to produce DEMs (Figure 3). In future analyses, we will examine more closely how to address the variation in vegetation and landscape through processing.

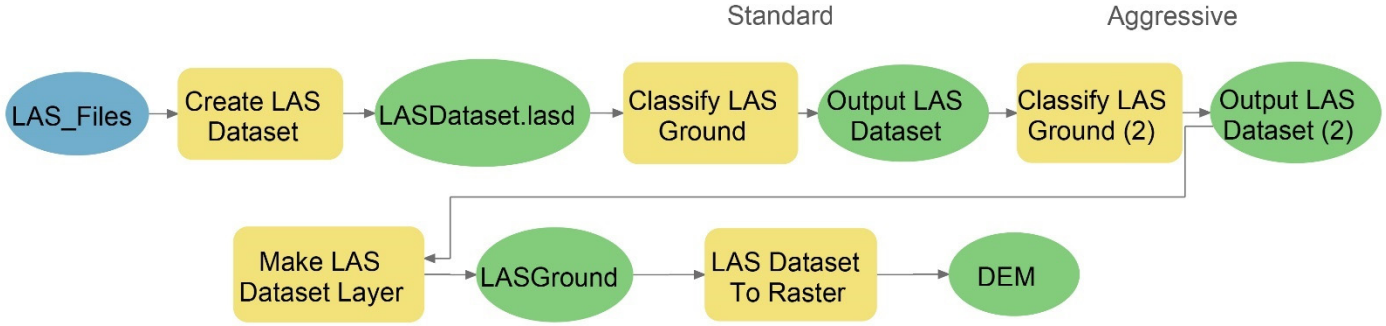

Figure 3. Workflow shown in ArcGIS Pro ModelBuilder for ground classification of LiDAR point clouds and generation of a digital elevation model.

Statistics are reported in Table 3 based on ground classification methods using ArcGIS Pro. Despite the variance in ground point classification from sample to sample, the resultant DEMs and visibility of archaeological remains did not vary greatly. Commission (type I) errors, in which vegetation was misclassified as ground, are more common overall in the data, especially in areas of dense low vegetation and drainages. Omission (type II) errors, in which actual ground points remained unclassified, are less common but appear in rugged terrain and in rare cases on the steepest hill summits. In order to define archaeological features, we relied first on surface models and simple raster derivatives, including hillshade, slope, and multidirectional hillshade; the first two generated with the Spatial Analyst toolbox in ArcGIS Pro and the third with the Relief Visualization Toolbox plugin in QGIS 3.16.6, with default parameters [73].

Here, we present the generated DEMs for each site without additional postprocessing. For archaeological purposes, we recommend starting with a standardized workflow such as the one we describe here to compare multiple sites. One long-term goal of our research is to experiment more systematically with several processing methods and algorithms to develop context-specific workflows that respond to the existing vegetation, topographic position, landform, and the scale and distribution of archaeological features [74–76].

Table 3. File statistics from the 6 UAV LiDAR missions.

Mission	# of .las Files	Total Points ($\times 10^7$)	Ground Points ($\times 10^7$)	Ground Points %	Area (km^2)	Ground Points/m^2	% 1st Return
Paso del Tigre	14	92.1	15.1	16.4	3.2	47	87.2
Canán	37	203.8	35.4	17.4	8.2	43	89.9
Edén-Jovero	16	116.6	17.4	15.0	3.3	52	88.0
El Pozo	14	109.5	4.4	4.0	2.8	15	77.1
Lacanjá Tzeltal	36	130.1	15.1	11.6	2.3	65	84.8
Benemérito Primera Sección	37	61.8	10.2	16.5	2.1	48	92.5

We discuss each of the six missions below in more detail, moving from north to south in the research area. Each mission was annotated to identify possible archaeological features, relying on a simple, basic definition of built or convex features (structures and agricultural terraces) and incised or concave features (*aguadas* or pits/reservoirs and channelized fields). Further characterization and ground verification of features is ongoing. Each mission represents a unique archaeological and environmental context, exhibiting different scales of settlement and modern land use, yet the results from the GatorEye surveys are consistent and demonstrate improvements from the 2017 and 2018 missions. These improvements are due to the higher total points collected, ranging from 610 million to 2 billion per mission in 2019, compared to 340–370 million points collected on each 2018 mission and 55 million points in the 2017 Piedras Negras mission. The increased point density was achieved by decreasing the distance between survey transects and increasing the number of possible flights with seven full sets of batteries. The upgraded sensor also allowed increased data collection while flying at higher overall altitudes. With this level of detail, our 2019 efforts confirm our previous estimate that 1–4 km^2 of area can be efficiently surveyed in a day [44,46], depending on mission planning and battery availability. We are confident that we can expand the area surveyed by widening the distance between flight transects, especially in areas that are cleared of secondary growth and with only moderate topographic variation.

3.1. Paso del Tigre, Las Limas, and Rancho Don Fermín

The first mission was located within the vicinity of the modern community of El Sacrificio, Palenque, Chiapas (Figure 4). This region consists of extensive or dispersed ancient Mayan settlements in an area of rolling hills today used primarily for agriculture and cattle grazing. The area is largely covered by low vegetation with pockets of secondary forest growth without a true canopy, increasing to the south in more rugged hills, with grassland being the primary type of land cover. Several archaeological sites have been recorded in this area, including the named sites of Paso del Tigre, Las Limas, and Rancho Don Fermín [77–79]. Previous excavations and ceramic analysis date occupation and use of Paso del Tigre from the Middle to Late Preclassic (500 BCE–250 CE) to the Late Classic (600–800 CE) periods, while Las Limas exhibits a single, shallow construction phase dating to the Late Classic (600–800 CE) period [80–83]. While Rancho Don Fermín has not been excavated and fully dated, surface collections of artifacts suggest at least a Preclassic period occupation, and we suspect a significant Classic period occupation as well.

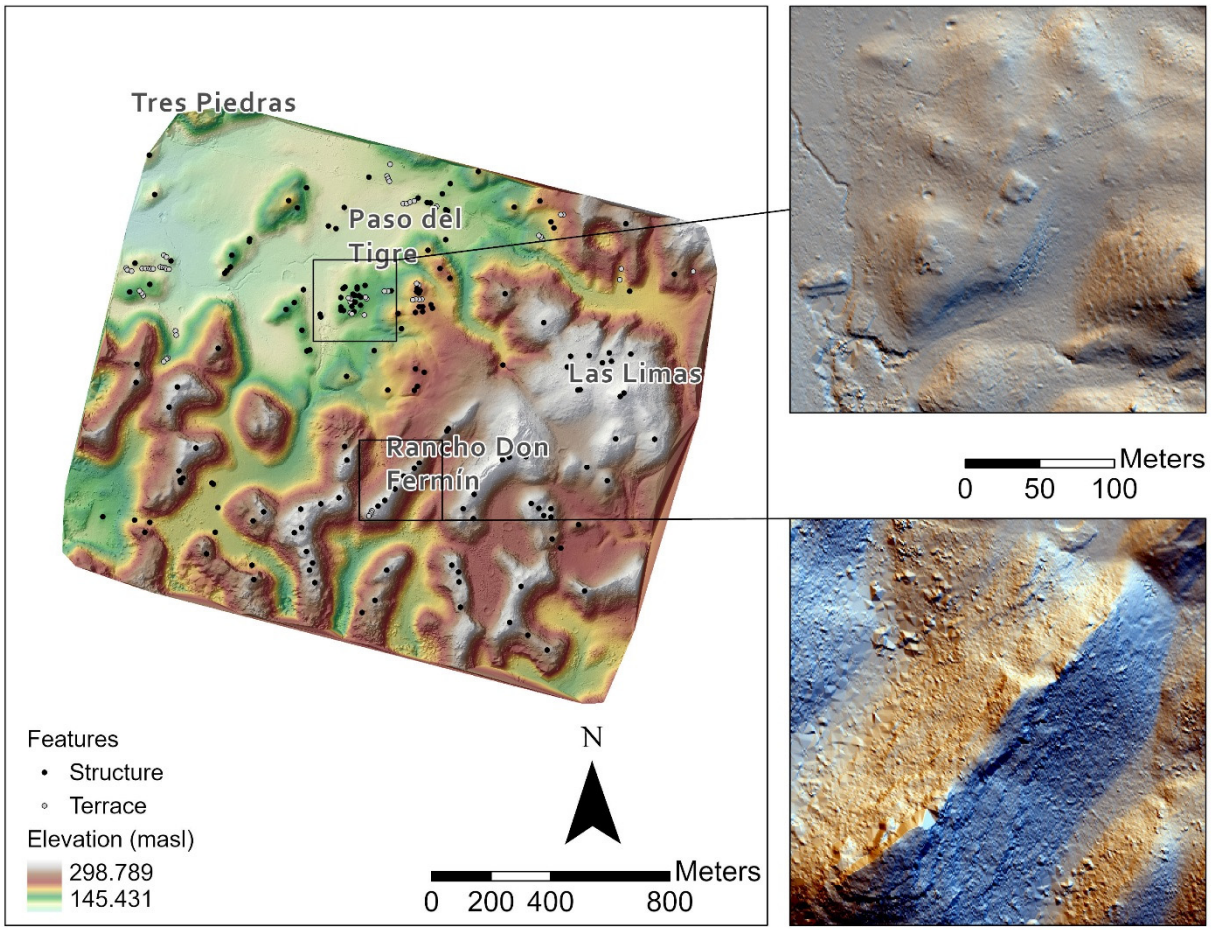

Figure 4. Processed DEM over hillshade of Paso del Tigre, Las Limas, and Rancho Don Fermín with identified features (left). Top inset shows a multidirectional hillshade of the Paso del Tigre site core and dam feature at left; bottom inset shows a multidirectional hillshade of structures along a narrow ridge and possible terracing at the southwest of the image at Rancho Don Fermín.

We documented 170 structures and 61 possible terraces within the mapped portion of the Paso del Tigre mission. Small structures known from ground survey are visible in raster derivatives of the DEM, including hillshade, but are challenging to identify without this ground knowledge; while smaller features are discernible, they are often indistinguishable from processing artifacts. Such artifacts are generally caused by misclassified vegetation in low ground point density areas, including along the edges of missions and on the slopes of steep drainages and hills.

Most of the archaeological remains are mounded foundations of house structures that once supported perishable superstructures. Las Limas and Paso del Tigre have denser concentrations of larger structures, or small site cores that represented the earliest settlement. The core of Paso del Tigre is notably larger with more diverse archaeological remains, including administrative and ritual architecture. Surrounding the core of Paso del Tigre, domestic structures are located on the summits of low hills, ringed by architectural terraces. A stream to the west of the Paso del Tigre core was also modified to impound water, with a dam span measuring 35 m long. The dam was clearly used over long periods because of its form and size relative to the small scale of the stream. Additionally, the area also contains a high number of reservoirs (regionally called aguadas) constructed for seasonal storage of water. These features are ubiquitous across the ancient and modern landscape and therefore require further ground verification to confirm their antiquity.

Rancho Don Fermín is located atop a steep but narrow (8–20 m wide) forested escarpment, which complicated ground classification. However, several large platforms and

terraces (previously known from ground surveys) are visible. Other nearby hilltops reveal similar modifications. This mission also documented the natural topography of this area, characterized by natural terraces formed by the erosion of the geological bedding planes. Although these features are natural, some were clearly modified to form architectural terraces, as documented at other sites across the region [84–86].

3.2. Nuevo Canán and Valle Escondido

This area incorporates two overlapping missions conducted over two separate, consecutive days (Figure 5). Flight lines captured portions of the modern communities of Nuevo Canán, Ocosingo; 11 de Julio, Palenque; and Rancho Vallescondido. Current land use consists primarily of grassland, with modern settlement, farmland, cattle grazing, and areas with medium to high canopy in the southwest approaching the hills that separate this valley from the adjacent Santo Domingo valley located further to the southwest. This southern portion of the mission represents the highest elevation change in the current study area, but the majority of the Nuevo Canán mission is characterized by flat wetland areas to the north of the modern highway. This mission contains one documented archaeological site named for the ranch of the same name, Valle Escondido, as well as a substantial network of drained fields in the seasonal swamps to the north of the modern highway [87,88]. The archaeological site of Valle Escondido consists of a series of platforms supporting a large, central structure and an ancillary structure with no evidence for domestic structures. The location affords a wide viewshed to the north, suggesting functions related to defense, a checkpoint, observation of agricultural fields, or a ritual function. Unfortunately, due to a field site location communication error, the GatorEye system did not collect any points over the Valle Escondido archaeological site; however, the surrounding hills show evidence of 46 structures or modifications with no clear core settlement. However, this region was likely used extensively for agriculture during the Classic Period, complemented by potential intensive agricultural features in the form of drained fields. Some terracing may be present in the hills surrounding Nuevo Canán, but as at Paso del Tigre, many of these features are likely natural bedding planes.

The most intensive zone of anthropogenic modification is located in the low-lying areas to the northeast of the modern community of Nuevo Canán. Over an area of at least 3 km^2, a large network of channelized fields drains seasonal swamps into permanent and intermittent streams for the purpose of maintaining and manipulating water table levels depending on seasonality. The antiquity of the features needs to be confirmed through excavation and analysis, as some were constructed historically or recently by members of the modern community. Channelized fields, however, appear distinct due to their consistent orientation (30° east of north) that does not conform to modern land use boundaries. The channels measure between 4 and 10 m wide by up to 120 m long and 20–30 cm deep, further revealing where modern irrigation canals intersect the older channels [88]. While further investigation is necessary to determine when these features were constructed, the detail provided by the LiDAR survey allows us to quantify field size and to estimate long-term productivity and sustainability.

3.3. El Edén and El Jovero

Located within land owned by residents of the modern settlement of Nuevo Guerrero, Ocosingo, El Edén and El Jovero were initially identified separately; however, LiDAR surveys demonstrate that if they are contemporary, they should be considered part of the same settlement cluster, representing one of the largest settlements in these study samples [89–91]. This mission contains a nearly equal proportion of forested to grassland area in an area of rolling hills. Low vegetation was misclassified to greater extent in this mission, especially along the edges of the survey and on the slopes of drainages. The El Edén–El Jovero settlement cluster consists of 236 structures identified in the GatorEye survey built on architectural terraces in an environment similar to Paso del Tigre (Figure 6). However, several areas exhibit formal architectural groups consisting of larger public and

plaza space, particularly three locations: (1) the area registered as the El Jovero site itself, (2) the area registered as the El Edén site, and (3) monumental architecture on a hill between the two sites.

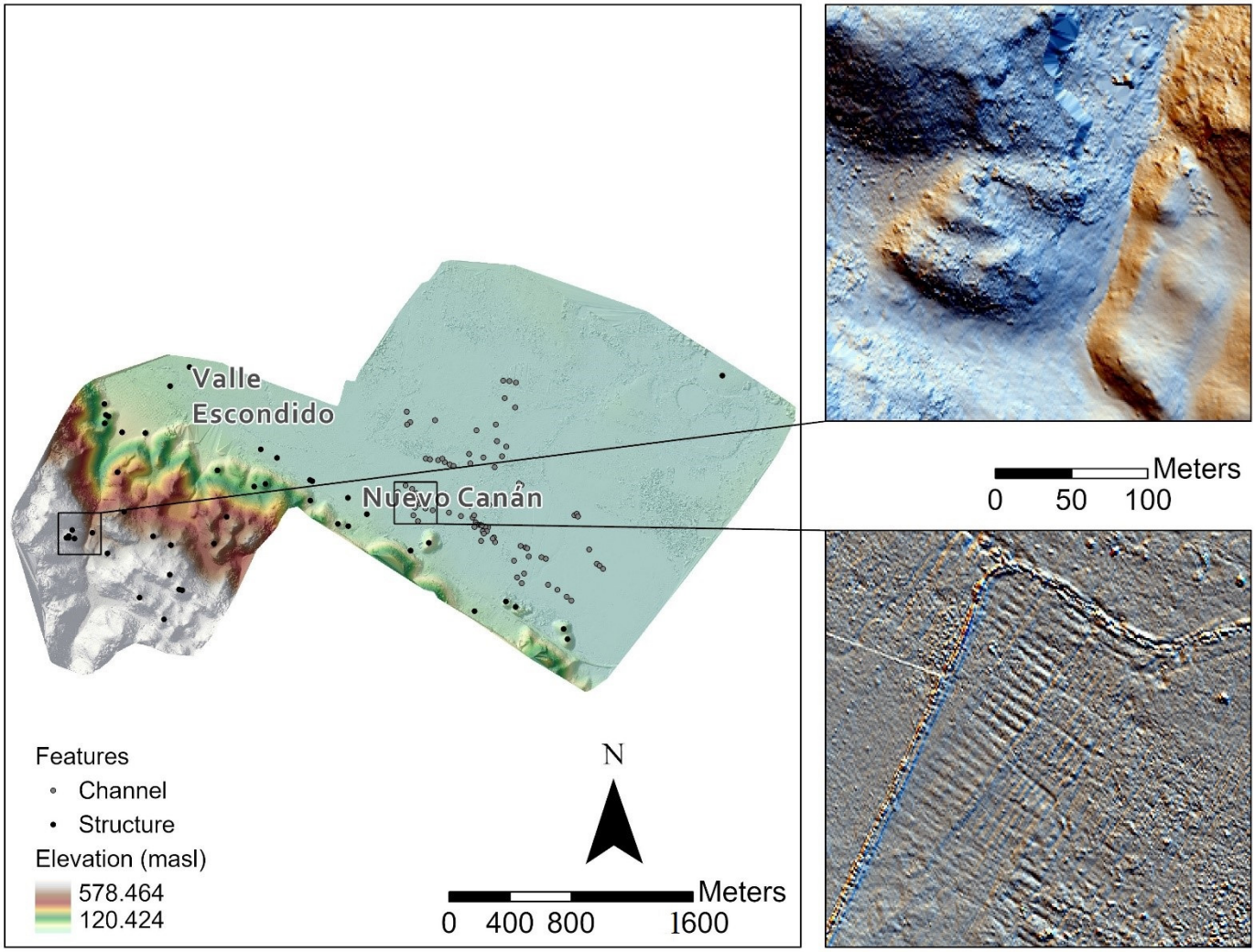

Figure 5. Processed DEM over hillshade of Nuevo Canán (left); points representing canals are not exhaustive and merely give a sense of the distribution of these linear features. Top inset shows a multidirectional hillshade of the rugged topography of steep slopes and deep gorges in the foothills to the southwest of the mapped area with possible structures; bottom inset shows a multidirectional hillshade of a portion of channelized fields alongside modern canals.

Other interesting features revealed in the GatorEye survey are the same extensive natural terraces known from Paso del Tigre; however, to a greater degree, El Edén and El Jovero show more evidence of anthropogenic terracing. Some terraces evidently bolstered the foundations of structures on hillsides. However, more abundant are distinctive terraces that follow the natural contours of the hills and do not support other architecture, which we infer to be constructed for agriculture. Such features were first noted in pedestrian surveys at El Edén in 2011 [89]. These terraces are difficult to quantify, as they are linear features and difficult to distinguish from natural bedding planes in the bedrock and "terracettes" formed by livestock, but we have identified at least 41 areas of terracing at El Edén–Jovero in the hills to the northeast and southeast of the El Jovero core.

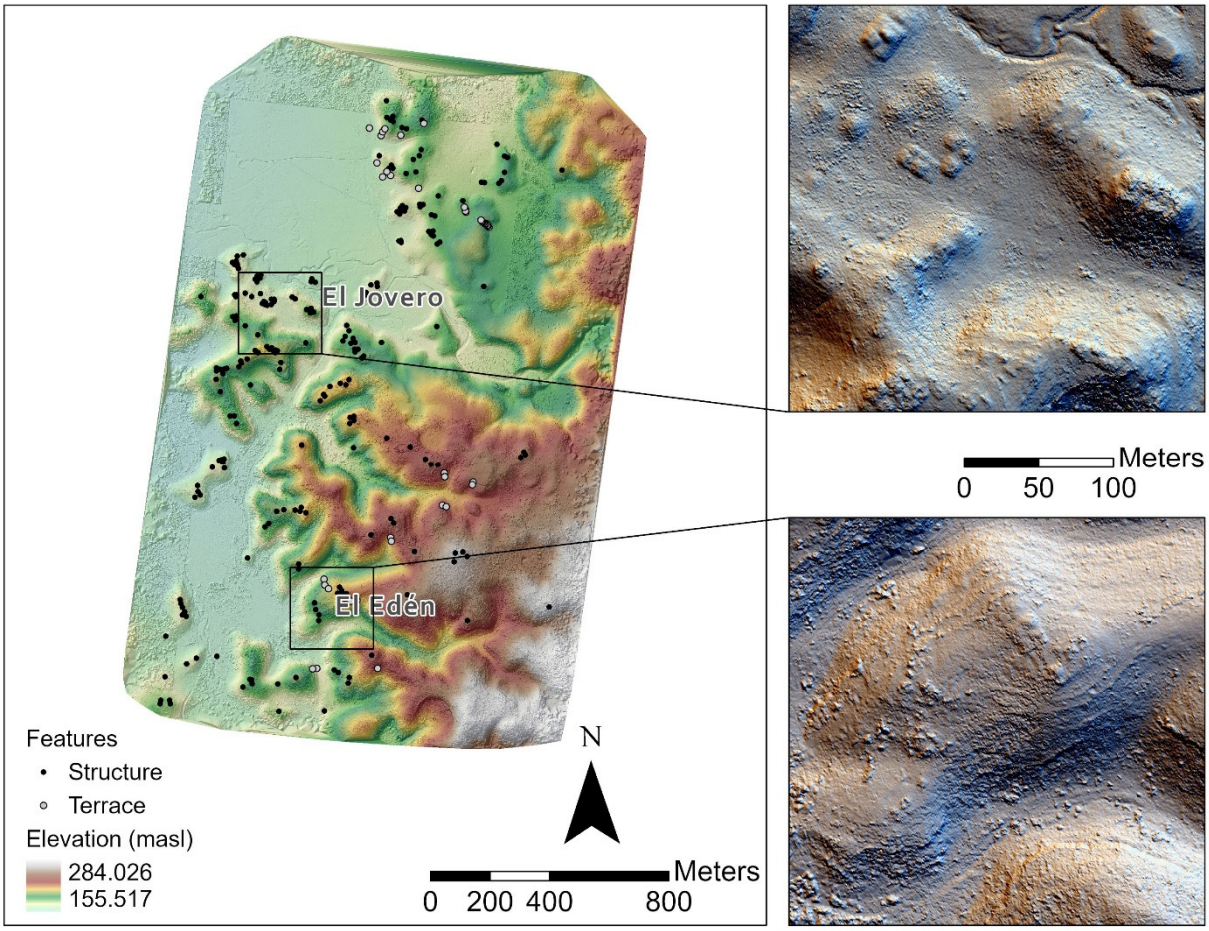

Figure 6. Processed DEM of El Edén and El Jovero; top inset shows the site core of El Jovero, bottom inset shows hilltop Scheme.

3.4. El Pozo de Nuevo Tumbalá

One of the most challenging missions in terms of ground classification was centered on the site of El Pozo de Nuevo Tumbalá (or El Pozo for short), named for a masonry cistern (or pozo in Spanish) built into an ancient hilltop platform and the eponymous nearby modern community. Approximately 90% of the surveyed area consists of medium to high canopy forest among rugged karst terrain consisting of steep cliffs and sinkholes, leading to a ground point percentage of 4.0%, the lowest of the 2019 missions (Figure 7). Due to the high pulse density of the UAV survey collected with overlapping flights, this low ground point percentage is enough to identify archaeological features in areas without steep terrain. However, in more rugged areas, archaeological features are difficult to distinguish without the context of ground-verified GPS points.

El Pozo is made up of settlement (27 structures identified with GatorEye) in low-lying valley areas, hilltops, and ridgelines, apparently with a low density of settlement features [85,92]. Large architecture as well as smaller domestic structures are present across the landscape in valley areas and elevated locations. Several possibly defensive walls line the approach to hilltop areas, but their small scale is generally not discernible in the LiDAR data. The highest escarpment is nearly inaccessible, surrounded by cliffs with a possible easier approach from the west. Despite its elevation, this escarpment contains several domestic structures, a large platform, and the cistern for which the site is named. This cistern is constructed of worked limestone blocks lined with stucco, similar to examples from house groups at Tecolote, Guatemala [93]. Despite El Pozo's proximity to surface water, the presence of a cistern within a platform on an inaccessible hilltop suggests a

concern with defense. Excavations at El Pozo confirmed a Late Classic period occupation based on ceramic analysis [94].

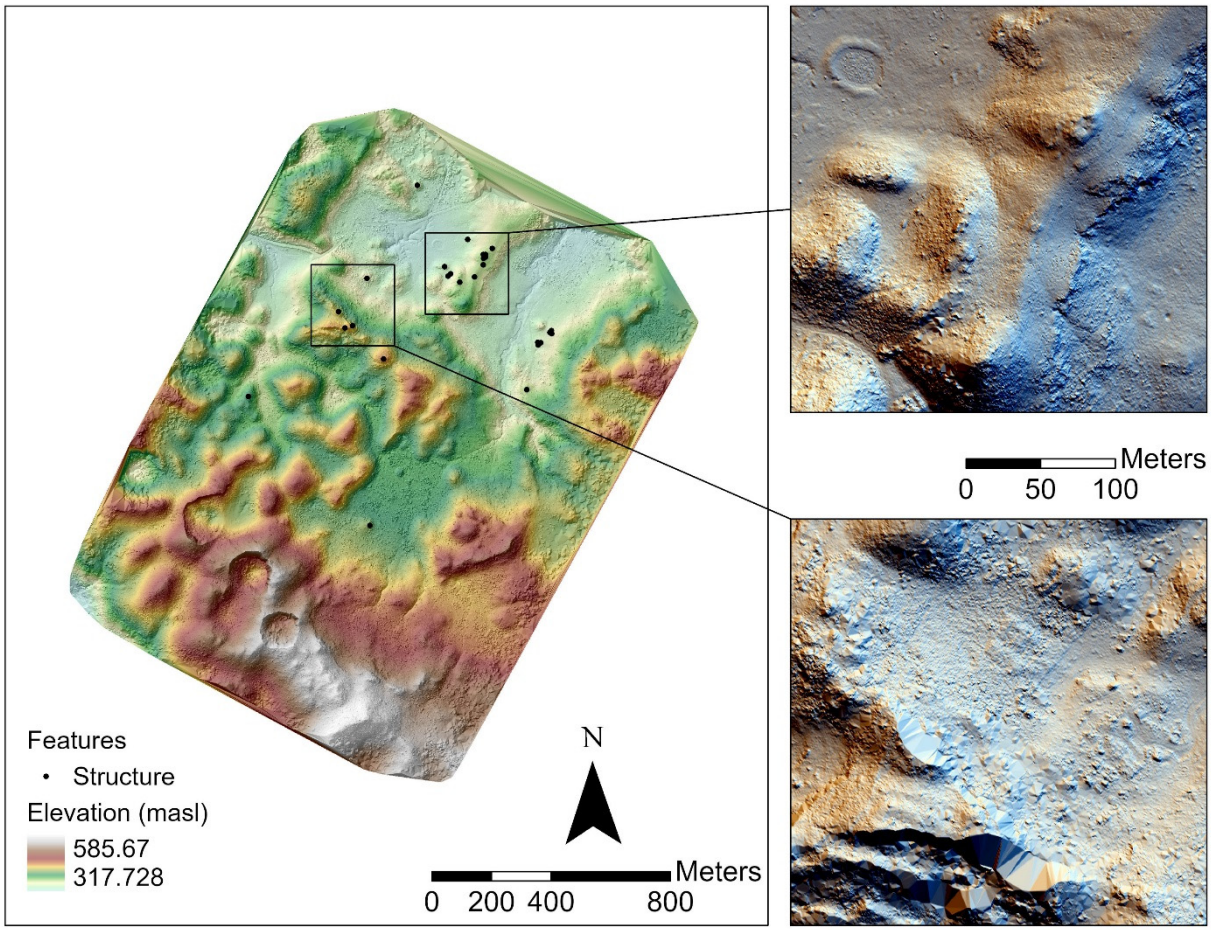

Figure 7. Processed DEM of El Pozo de Nuevo Tumbalá, the top inset shows hilltop settlement, the bottom inset shows poor ground classification of the steep escarpment overlooking the valley portion of the site to the north.

3.5. Lacanjá Tzeltal

The archaeological site of Lacanjá Tzeltal is located near the headwaters of the Lacanja River and during the Late Classic period was a capital of the Sak Tz'i, a kingdom ruled by a dynasty best known from looted monuments and textual references found on inscriptions at other sites in the Western Maya Lowlands [95–98]. Lacanjá Tzeltal has been mapped with terrestrial methods (including tape-and-compass and total station), UAV photogrammetry, and occupied airborne LiDAR collected by the National Center for Airborne Laser Mapping (NCALM) [58], thus offering the most comparative data to compare with the results from the GatorEye system (Figure 8). These spatial data are complemented by several field seasons of excavation that have documented occupation from at least 750 BCE through the 9th century CE [99–101]. The valley setting affords a relatively flat landscape bounded by low hills to the southwest of the site core, with grassland representing the primary land cover category. Several small tributaries of the Lacanja River carve gorges through the site, especially on the northwest edge of the core. The data collected by GatorEye thus provide an opportunity to model the location's hydrology and how architecture has modified the flow of water. The map also shows that the site is compact with only scattered house groups on the hills surrounding the site core, totaling 195 structures within the mapped extent.

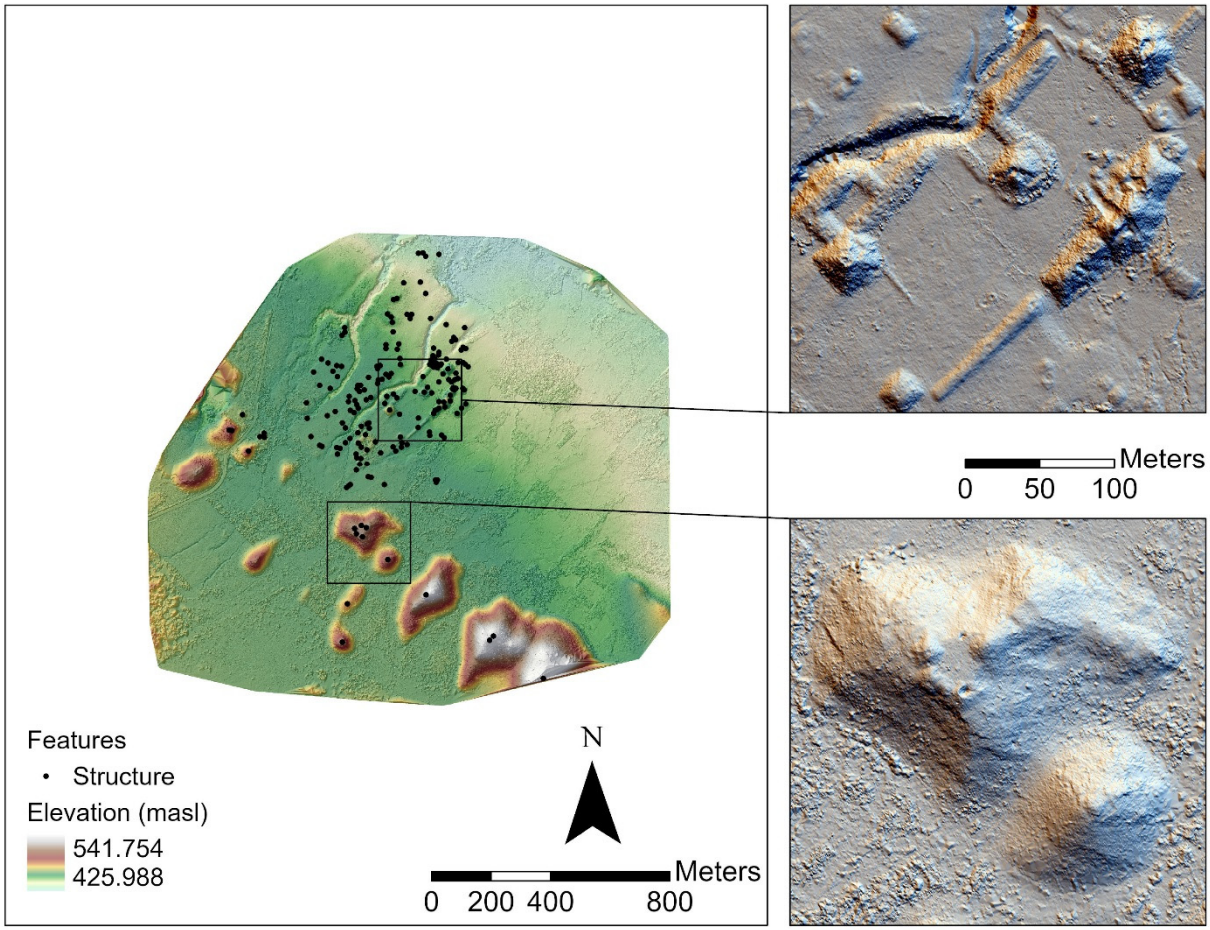

Figure 8. Processed DEM of Lacanjá Tzeltal. The top inset shows the monumental core of the site; the bottom inset shows a hilltop architectural group to the south.

3.6. Benemérito de las Américas, Primera Sección

The final mission discussed in this paper is 80 km south of the other areas mapped in 2019. This mission was flown over the archaeological site of Benemérito de las Américas, Primera Sección, a large ancient Maya center located near the confluence of the Upper Usumacinta and Lacantún Rivers [102–104] (Figure 9). Excavations and surface collection have recovered ceramics dating to the Terminal Classic period (830–950 CE), although the volume of construction supports the likelihood of earlier occupations, certainly during the Classic period, if not earlier [105,106]. As at Lacanjá Tzeltal, the setting is predominantly flat and cleared of vegetation, except for portions of the north–south trending ridge that contain most of the monumental site core. Settlement, however, extends toward the edges of the mapped area along the ridge's spurs. The settlement is notably dense, including 771 structures identified in the GatorEye data, oriented around the main ridge or acropolis. In outlying areas of the site, these structures cluster around 43 household aguadas, or reservoirs, also used as borrow pits for building material.

Comparative data is also available at Benemérito Primera Sección, collected by NASA Goddard's LiDAR, Hyperspectral, and Thermal Imager (G-LiHT), which documented part of the site core in a narrow, 300 m wide LiDAR transect [12,38,70,107]. Although this transect covered a limited portion of the site, the ground point density (74.0%) was far higher than that of the 2019 GatorEye mission (16.5%), likely due to differences in processing, the fact that the GatorEye mapped area contained more medium to high forest, and that the GatorEye mission took place during the rainy season (June) compared to the G-LiHT data, which was collected at the end of the dry season (April), leading to difficulties in classifying ground points under low vegetation in the GatorEye sample.

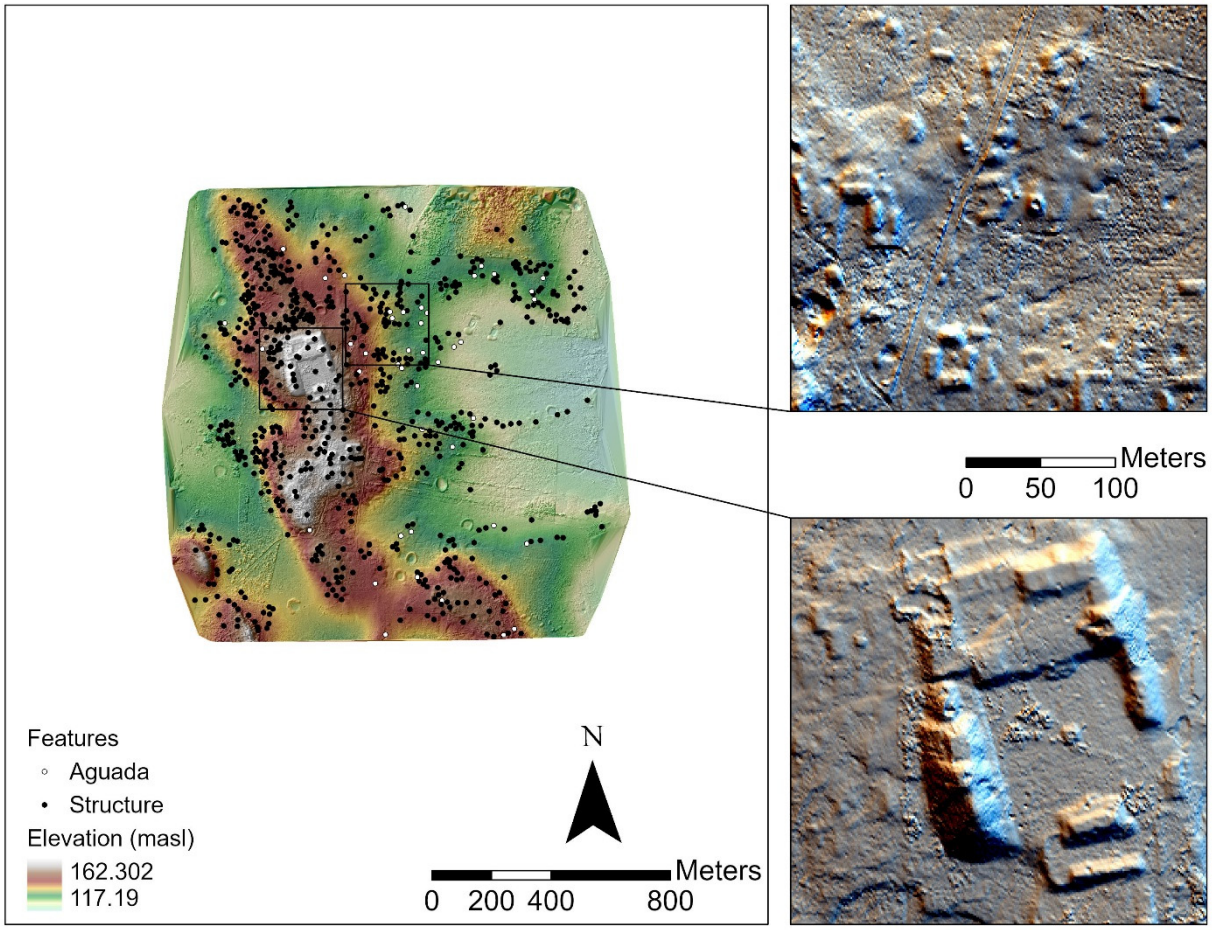

Figure 9. Processed DEM of Benemérito Primera Sección. The top inset shows abundant domestic patio groups surrounding aguadas or reservoirs; the bottom inset shows the main plaza and acropolis of the site.

4. Discussion

UAV LiDAR offers unique scientific utility for capturing detailed information about ancient landscapes and settlements as an in-field archaeological tool with significant advantages over occupied airborne or satellite systems in portability, operational costs, and replicability. Over the past four years, we have been testing and refining our field data collection and processing to better develop systematic methods for documenting these landscapes. We have shown that in diverse and complex modern land use regimes, with proper mission planning, UAV LiDAR can be used to map targeted areas. Local knowledge of the landscape through previous ground-based survey and collaboration with communities offers a critical context to properly conduct such missions. Furthermore, such data do not require (although they will certainly benefit from) complex processing pipelines. Instead, UAV LiDAR data can be processed through straightforward, automated software such as ArcGIS Pro.

Alongside successful mapping of several archaeological sites in the Upper Usumacinta region, our findings are of broader use to archaeologists interested in planning UAV LiDAR missions in the context of complex modern land use regimes and topographic variation (Table 4). As expected, vegetation coverage, calculated as a ratio of forest to grassland from land cover classification of 2019 satellite imagery, influences ground classification with lower ground point percentage in areas with more forest (Figure 10). However, when eliminating El Pozo as an outlier, more variation is clear, signaling that other factors influenced ground classification. A more detailed classification of vegetation type, for example, primary vs. secondary growth, vegetation stress, and canopy height, among others, would likely reveal clearer patterns.

Table 4. Summary of forest–grassland ratio, mean absolute curvature of 10 m resolution surfaces resampled from the LiDAR bare earth models and edge-corrected, ground point percentage, and feature point density per square kilometer. Higher mean absolute curvatures are an index of higher topographic ruggedness.

Site	Forest: Grassland Ratio	Mean Absolute Curvature	Ground Point Percentage	Feature Density per km^2
Paso del Tigre	0.722	2.15	16.4	72
Benemérito Primera Sección	0.0271	0.56	16.5	388
Edén-Jovero	1.01	1.35	15.0	84
El Pozo	6.49	2.34	4.0	10
Lacanjá Tzeltal	0.766	1.13	11.6	85
Nuevo Canán	0.660	0.82	17.4	16

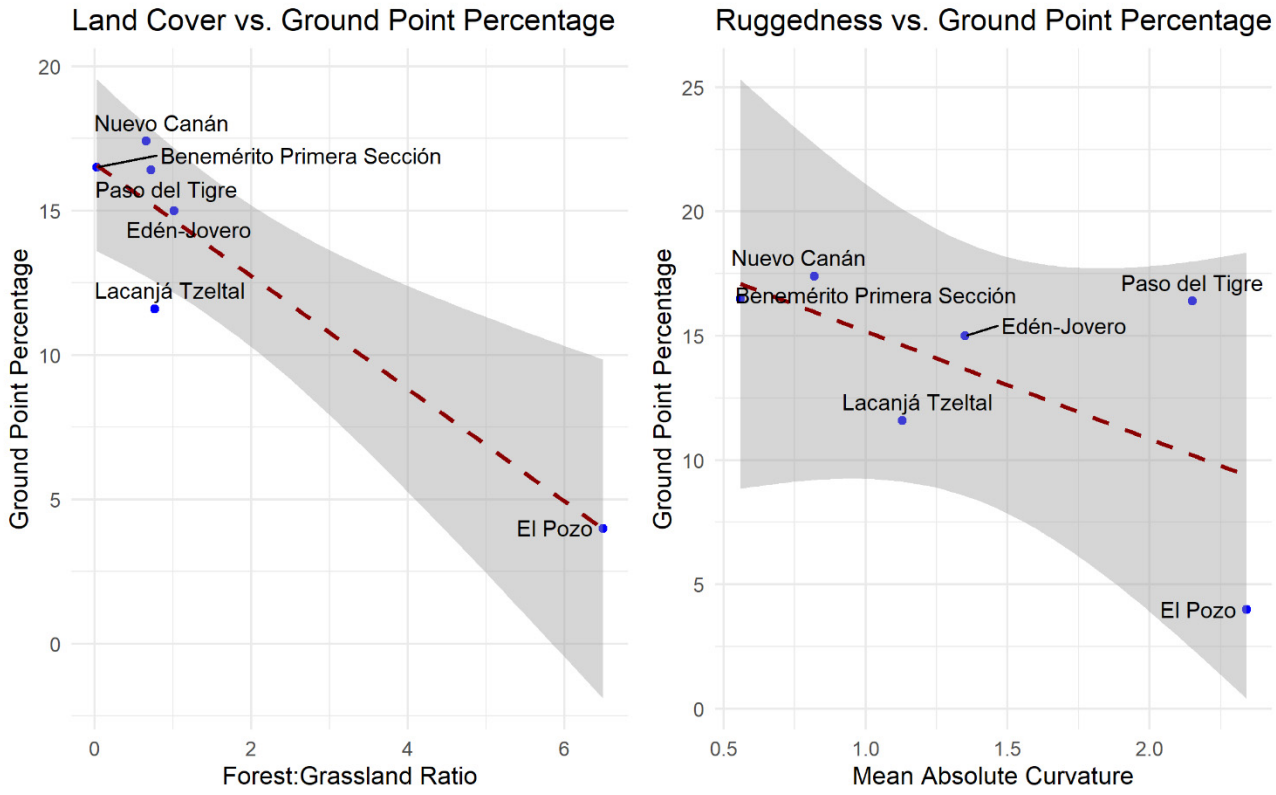

Figure 10. Scatter plots with trend lines and confidence intervals showing the relationship between ground point percentage and land cover or ruggedness, respectively.

Terrain ruggedness is an additional challenge in the Upper Usumacinta study region, both in the need for higher point densities to model abrupt topographic change as well as in the additional complications in accurately filtering ground points on high slopes without misclassifying vegetation. We have observed that the most challenging feature identification takes place in a combination of rugged terrain and forest cover [108,109]. For example, although Paso del Tigre and El Pozo have similar levels of ruggedness based on mean absolute curvature (the second derivative of the DEM) [110], the low forest to grassland ratio at Paso del Tigre led to a higher ground point percentage. These issues are not unique to UAV LiDAR, however, as we face the same difficulties in the study region with occupied airborne LiDAR data [58]. A further benefit of UAV LiDAR surveys is that point returns can be densified simply with additional flights or increasing the overlap between transects. Indeed, the mission with the lowest ground point density in this case study, El Pozo, with 4.0% ground points still produced a density of 16 ground points per square meter, which is more than enough for the generation of bare earth models. We did

not detect a strong correlation between ground point density and feature density, although future ground verification, particularly at El Pozo, will be required to identify the presence of false negatives to establish whether low feature density there is due to settlement choices or the resolution of the data. With future missions, we may be able to identify land cover and ruggedness thresholds where ground point percentage drops significantly.

5. Conclusions

While UAV LiDAR does not provide the same regional coverage that occupied airborne LiDAR offers, it provides a detailed perspective through high-precision mapping to identify archaeological features across the landscape. Importantly, our surveys allow us to move beyond general questions about the presence or absence of ancient settlement. We can begin to piece together the complex coupled natural and human systems that were operating across many centuries with the added potential of tracking seasonal and yearly changes in these systems with follow-up missions. Agrarian features, domestic architecture, reservoirs, and public architecture are dispersed in a mosaic across the landscape, and UAV LiDAR provides detailed samples that we can now use to study how this mosaic influenced past land use and how past land use influences current land use and natural systems, such as hydrology. A more detailed perspective can benefit from complementary field survey to better interpret the outcomes from UAV mapping.

In summary, the improvements in data outcomes from 2017 to 2019 demonstrate that results benefit from additional mission planning, experience, and technological upgrades. Importantly, UAV LiDAR requires complementary fieldwork and in this case study has benefitted from the decade of research and community relationship development that preceded the UAV flights. We reiterate that UAV LiDAR systems are not a replacement for occupied airborne LiDAR, but rather offer a complementary and independent tool that will strengthen archaeological science, especially when investigating ancient coupled natural and human systems. UAV offers many advantages, including our ability to collect data over the same area across different seasons or over multiple years to monitor changes to archaeological resources, vegetation, land use, and natural systems. As the landscape evolves, we will simply return to these sites to document how these landscapes change through time. Finally, with minimal preprocessing, we are collecting more points than necessary, and future analyses will assess to what degree point thinning affects results. Identifying the costs and benefits of high point densities, in terms of collection costs, storage, processing, and feature identification, will be pursued in future research. Nevertheless, these data offer new collaborative opportunities to expand the use and application of these data with soil scientists, ecologists, and land use scientists. While the archaeological features are exciting, potentially more promising are the developing research teams to examine the full history of land use and settlement in this region to more fully document and learn from changing patterns of community and landscape across the southern lowlands of Mexico.

Author Contributions: Conceptualization, W.S., T.M., C.G., A.K.S., E.N.B., A.M.A.Z., K.H., R.G.; methodology, W.S., T.M., C.G., A.K.S., E.N.B., A.M.A.Z., K.H., R.G.; formal analysis, W.S., T.M., K.H.; investigation W.S., T.M., C.G., A.K.S., E.N.B., A.M.A.Z., K.H., R.G.; writing—original draft preparation, W.S. and T.M.; writing—review and editing, W.S., T.M., C.G., E.N.B., R.G.; funding acquisition, T.M., C.G., A.K.S. All authors have read and agreed to the published version of the manuscript.

Funding: This research was funded by the Alphawood Foundation of Chicago, the National Science Foundation (BCS-1917671), and NASA (80NSSC20K1265).

Institutional Review Board Statement: Not applicable.

Informed Consent Statement: Not applicable.

Data Availability Statement: Data are available for viewing purposes at http://www.speclab.org/gatoreye-data-access.html (accessed on 18 November 2021). Uses other than viewing may be discussed with the authors and GatorEye co-directors.

Acknowledgments: This research was approved by Instituto Nacional de Antropología e Historia (INAH, Mexico) and the local communities and landowners. We thank the McIntire–Stennis program of the USDA for support towards the GatorEye program development and implementation.

Conflicts of Interest: The authors declare no conflict of interest. The funders had no role in the design of the study; in the collection, analyses, or interpretation of data; in the writing of the manuscript, or in the decision to publish the results.

References

1. Canuto, M.A.; Estrada-Belli, F.; Garrison, T.G.; Houston, S.D.; Acuña, M.J.; Kováč, M.; Marken, D.; Nondédéo, P.; Auld-Thomas, L.; Castanet, C.; et al. Ancient lowland Maya complexity as revealed by airborne laser scanning of northern Guatemala. *Science* **2018**, *361*, eaau0137. [CrossRef] [PubMed]
2. Chase, A.F.; Chase, D.Z.; Weishampel, J.F.; Drake, J.B.; Shrestha, R.L.; Slatton, K.C.; Awe, J.J.; Carter, W.E. Airborne LiDAR, archaeology, and the ancient Maya landscape at Caracol, Belize. *J. Archaeol. Sci.* **2011**, *38*, 387–398. [CrossRef]
3. Chase, A.F.; Chase, D.Z.; Fisher, C.T.; Leisz, S.J.; Weishampel, J.F. Geospatial revolution and remote sensing LiDAR in Mesoamerican archaeology. *Proc. Natl. Acad. Sci. USA* **2012**, *109*, 12916–12921. [CrossRef] [PubMed]
4. Hutson, S.R. Adapting LiDAR data for regional variation in the tropics: A case study from the Northern Maya Lowlands. *J. Archaeol. Sci. Rep.* **2015**, *4*, 252–263. [CrossRef]
5. Inomata, T.; Triadan, D.; Pinzón, F.; Aoyama, K. Artificial plateau construction during the Preclassic period at the Maya site of Ceibal, Guatemala. *PLoS ONE* **2019**, *14*, e0221943. [CrossRef]
6. Inomata, T.; Triadan, D.; López, V.A.V.; Fernandez-Diaz, J.C.; Omori, T.; Bauer, M.B.M.; Hernández, M.G.; Beach, T.; Cagnato, C.; Aoyama, K.; et al. Monumental architecture at Aguada Fénix and the rise of Maya civilization. *Nature* **2020**, *582*, 530–533. [CrossRef]
7. Inomata, T.; Fernandez-Diaz, J.C.; Triadan, D.; Mollinedo, M.G.; Pinzón, F.; Hernández, M.G.; Flores, A.; Sharpe, A.; Beach, T.; Hodgins, G.W.L.; et al. Origins and spread of formal ceremonial complexes in the Olmec and Maya regions revealed by airborne lidar. *Nat. Hum. Behav.* **2021**, *5*, 1487–1501. [CrossRef]
8. Ringle, W.M.; Negrón, T.G.; Ciau, R.M.; Seligson, K.E.; Fernandez-Diaz, J.C.; Zapata, D.O. Lidar survey of ancient Maya settlement in the Puuc region of Yucatan, Mexico. *PLoS ONE* **2021**, *16*, e0249314. [CrossRef]
9. Rosenswig, R.M.; López-Torrijos, R.; Antonelli, C.E.; Mendelsohn, R.R. Lidar mapping and surface survey of the Izapa state on the tropical piedmont of Chiapas, Mexico. *J. Archaeol. Sci.* **2013**, *40*, 1493–1507. [CrossRef]
10. Canuto, M.A.; Auld-Thomas, L. Taking the high ground: A model for lowland Maya settlement patterns. *J. Anthr. Archaeol.* **2021**, *64*, 101349. [CrossRef]
11. Chase, A.F.; Chase, D.Z.; Weishampel, J.F. Lasers in the Jungle. *Archaeology* **2010**, *63*, 27–29.
12. Schroder, W.; Murtha, T.; Golden, C.; Hernández, A.A.; Scherer, A.; Morell-Hart, S.; Almeida Zambrano, A.; Broadbent, E.; Brown, M. The lowland Maya settlement landscape: Environmental LiDAR and ecology. *J. Archaeol. Sci. Rep.* **2020**, *33*, 102543. [CrossRef]
13. Chase, A.; Weishampel, J. Using Lidar and GIS to Investigate Water and Soil Management in the Agricultural Terracing at Caracol, Belize. *Adv. Archaeol. Pract.* **2016**, *4*, 357–370. [CrossRef]
14. Inomata, T.; Pinzón, F.; Ranchos, J.L.; Haraguchi, T.; Nasu, H.; Fernandez-Diaz, J.C.; Aoyama, K.; Yonenobu, H. Archaeological Application of Airborne LiDAR with Object-Based Vegetation Classification and Visualization Techniques at the Lowland Maya Site of Ceibal, Guatemala. *Remote Sens.* **2017**, *9*, 563. [CrossRef]
15. Inomata, T.; Triadan, D.; Pinzón, F.; Burham, M.; Ranchos, J.L.; Aoyama, K.; Haraguchi, T. Archaeological application of airborne LiDAR to examine social changes in the Ceibal region of the Maya lowlands. *PLoS ONE* **2018**, *13*, e0191619. [CrossRef]
16. Weishampel, J.F.; Chase, A.F.; Chase, D.Z.; Drake, J.B.; Shrestha, R.L.; Slatton, K.C.; Awe, J.J.; Hightower, J.; Angelo, J. Remote sensing of ancient Maya land use features at Caracol, Belize related to tropical rainforest structure. In *Space, Time, Place: Third International Conference on Remote Sensing Archaeology*; Forte, M., Campana, S., Liuzza, C., Eds.; British Archaeological Reports S2118: Oxford, UK, 2010; Volume 2118, pp. 45–52.
17. Doneus, M.; Briese, C. Full-Waveform Airborne Laser Scanning as a Tool for Archaeological Reconnaissance. In *From Space to Place: 2nd International Conference on Remote Sensing in Archaeology, Proceedings of the 2nd International Workshop, CNR, Rome, Italy, 4–7 December 2006*; Campana, S., Forte, M., Eds.; BAR Publishing: Oxford, UK, 2006; pp. 99–105.
18. Doneus, M.; Briese, C.; Fera, M.; Janner, M. Archaeological prospection of forested areas using full-waveform airborne laser scanning. *J. Archaeol. Sci.* **2008**, *35*, 882–893. [CrossRef]
19. Corte, A.P.D.; Rex, F.E.; de Almeida, D.R.A.; Sanquetta, C.R.; Silva, C.A.; Moura, M.M.; Wilkinson, B.; Zambrano, A.M.A.; da Cunha Neto, E.M.; Veras, H.F.P.; et al. Measuring Individual Tree Diameter and Height Using GatorEye High-Density UAV-Lidar in an Integrated Crop-Livestock-Forest System. *Remote Sens.* **2020**, *12*, 863. [CrossRef]
20. Corte, A.P.D.; Souza, D.V.; Rex, F.E.; Sanquetta, C.R.; Mohan, M.; Silva, C.A.; Zambrano, A.M.A.; Prata, G.; de Almeida, D.R.A.; Trautenmüller, J.W.; et al. Forest inventory with high-density UAV-Lidar: Machine learning approaches for predicting individual tree attributes. *Comput. Electron. Agric.* **2020**, *179*, 105815. [CrossRef]
21. Kellner, J.R.; Armston, J.; Birrer, M.; Cushman, K.C.; Duncanson, L.; Eck, C.; Falleger, C.; Imbach, B.; Král, K.; Krůček, M.; et al. New Opportunities for Forest Remote Sensing Through Ultra-High-Density Drone Lidar. *Surv. Geophys.* **2019**, *40*, 959–977. [CrossRef]

22. Lin, Y.-C.; Cheng, Y.-T.; Zhou, T.; Ravi, R.; Hasheminasab, S.M.; Flatt, J.E.; Troy, C.; Habib, A. Evaluation of UAV LiDAR for Mapping Coastal Environments. *Remote Sens.* **2019**, *11*, 2893. [CrossRef]
23. Prata, G.; Broadbent, E.; De Almeida, D.; Peter, J.; Drake, J.; Medley, P.; Corte, A.; Vogel, J.; Sharma, A.; Silva, C.; et al. Single-Pass UAV-Borne GatorEye LiDAR Sampling as a Rapid Assessment Method for Surveying Forest Structure. *Remote Sens.* **2020**, *12*, 4111. [CrossRef]
24. Resop, J.P.; Lehmann, L.; Hession, W.C. Drone Laser Scanning for Modeling Riverscape Topography and Vegetation: Comparison with Traditional Aerial Lidar. *Drones* **2019**, *3*, 35. [CrossRef]
25. Sofonia, J.J.; Phinn, S.; Roelfsema, C.; Kendoul, F.; Rist, Y. Modelling the effects of fundamental UAV flight parameters on LiDAR point clouds to facilitate objectives-based planning. *ISPRS J. Photogramm. Remote Sens.* **2019**, *149*, 105–118. [CrossRef]
26. Wallace, L.; Lucieer, A.; Watson, C.; Turner, D. Development of a UAV-LiDAR System with Application to Forest Inventory. *Remote Sens.* **2012**, *4*, 1519–1543. [CrossRef]
27. Bikoulis, P.; Gonzalez-Macqueen, F.; Spence-Morrow, G.; Álvarez, W.Y.; Bautista, S.; Jennings, J. A new methodology for geoglyph research: Preliminary survey results and practical workflow from the Quilcapampa Geoglyph Survey (Sihuas Valley, Peru). *J. Archaeol. Sci. Rep.* **2016**, *10*, 119–129. [CrossRef]
28. Chiabrando, F.; D'Andria, F.; Sammartano, G.; Spanò, A. UAV photogrammetry for archaeological site survey. 3D models at the Hierapolis in Phrygia (Turkey). *Virtual Archaeol. Rev.* **2018**, *9*, 28–43. [CrossRef]
29. Field, S.; Waite, M.; Wandsnider, L. The utility of UAVs for archaeological surface survey: A comparative study. *J. Archaeol. Sci. Rep.* **2017**, *13*, 577–582. [CrossRef]
30. Hill, A.C. Economical drone mapping for archaeology: Comparisons of efficiency and accuracy. *J. Archaeol. Sci. Rep.* **2019**, *24*, 80–91. [CrossRef]
31. Kadhim, I.; Abed, F.M. The Potential of LiDAR and UAV-Photogrammetric Data Analysis to Interpret Archaeological Sites: A Case Study of Chun Castle in South-West England. *ISPRS Int. J. Geo-Inf.* **2021**, *10*, 41. [CrossRef]
32. Magnani, M.; Douglass, M.; Schroder, W.; Reeves, J.; Braun, D.R. The Digital Revolution to Come: Photogrammetry in Archaeological Practice. *Am. Antiq.* **2020**, *85*, 737–760. [CrossRef]
33. Marín-Buzón, C.; Pérez-Romero, A.; López-Castro, J.; Ben Jerbania, I.; Manzano-Agugliaro, F. Photogrammetry as a New Scientific Tool in Archaeology: Worldwide Research Trends. *Sustainability* **2021**, *13*, 5319. [CrossRef]
34. Nikolakopoulos, K.G.; Soura, K.; Koukouvelas, I.K.; Argyropoulos, N.G. UAV vs. classical aerial photogrammetry for archaeological studies. *J. Archaeol. Sci. Rep.* **2017**, *14*, 758–773. [CrossRef]
35. Olson, K.G.; Rouse, L.M. A Beginner's Guide to Mesoscale Survey with Quadrotor-UAV Systems. *Adv. Archaeol. Pract.* **2018**, *6*, 357–371. [CrossRef]
36. Rouse, L.M.; Krumnow, J. On the fly: Strategies for UAV-based archaeological survey in mountainous areas of Central Asia and their implications for landscape research. *J. Archaeol. Sci. Rep.* **2020**, *30*, 102275. [CrossRef]
37. Carmona, J.S.; Quirós, E.; Mayoral, V.; Charro, C. Assessing the potential of multispectral and thermal UAV imagery from archaeological sites. A case study from the Iron Age hillfort of Villasviejas del Tamuja (Cáceres, Spain). *J. Archaeol. Sci. Rep.* **2020**, *31*, 102312. [CrossRef]
38. Schroder, W.; Golden, C.; Scherer, A.; Murtha, T.; Firpi, O. Remote Sensing and Reconnaissance along the Lacantún River: The Lakamtuun Dynasty and the Sites of El Palma and Benemérito de Las Américas, Primera Sección. *Mexicon* **2019**, *41*, 157–167.
39. Vilbig, J.M.; Sagan, V.; Bodine, C. Archaeological surveying with airborne LiDAR and UAV photogrammetry: A comparative analysis at Cahokia Mounds. *J. Archaeol. Sci. Rep.* **2020**, *33*, 102509. [CrossRef]
40. Barbour, T.E.; Sassaman, K.E.; Zambrano, A.M.A.; Broadbent, E.N.; Wilkinson, B.; Kanaski, R. Rare pre-Columbian settlement on the Florida Gulf Coast revealed through high-resolution drone LiDAR. *Proc. Natl. Acad. Sci. USA* **2019**, *116*, 23493–23498. [CrossRef]
41. Poirier, N.; Baleux, F.; Calastrenc, C. The Mapping of Forested Archaeological Sites Using UAV LiDaR. A Feedback from a South-West France Experiment in Settlement & Landscape Archaeology. *Digit. Archaeol.* **2020**, *4*, 1–24. [CrossRef]
42. Ćmielewski, B.; Sieczkowska, D.; Kościuk, J.; Bastante, J.M.; Wilczyńska, I. UAV LiDAR Mapping in the Historic Sanctuary of Machupicchu: Challenges and Preliminary Results: Part 1. Wiadomości Konserwatorskie. *J. Herit. Conserv.* **2021**, *67*, 159–170. [CrossRef]
43. McCoy, M.D.; Casana, J.; Hill, A.C.; Laugier, E.J.; Mulrooney, M.A.; Ladefoged, T.N. Unpiloted Aerial Vehicle Acquired Lidar for Mapping Monumental Architecture: A Case Study from the Hawaiian Islands. *Adv. Archaeol. Pract.* **2021**, *9*, 160–174. [CrossRef]
44. Murtha, T.M.; Broadbent, E.N.; Golden, C.; Scherer, A.; Schroder, W.; Wilkinson, B.; Zambrano, A.A. Drone-Mounted Lidar Survey of Maya Settlement and Landscape. *Lat. Am. Antiq.* **2019**, *30*, 630–636. [CrossRef]
45. Risbøl, O.; Gustavsen, L. LiDAR from drones employed for mapping archaeology—Potential, benefits and challenges. *Archaeol. Prospect.* **2018**, *25*, 329–338. [CrossRef]
46. Schroder, W.; Murtha, T.; Broadbent, E.N.; Zambrano, A.M.A. A confluence of communities: Households and land use at the junction of the Upper Usumacinta and Lacantún Rivers, Chiapas, Mexico. *World Archaeol.* **2021**, 1–28. [CrossRef]
47. Van Valkenburgh, P.; Cushman, K.C.; Castillo Butters, L.J.; Rojas Vega, C.; Roberts, C.; Kepler, C.; Kellner, J. Lasers Without Lost Cities: Using Drone Lidar to Capture Architectural Complexity at Kuelap, Amazonas, Peru. *J. Field Archaeol.* **2020**, *45*, S75–S88. [CrossRef]

48. Comer, D.C.; Comer, J.A.; Dumitru, I.A.; Ayres, W.S.; Levin, M.J.; Seikel, K.A.; White, D.A.; Harrower, M.J. Airborne LiDAR Reveals a Vast Archaeological Landscape at the Nan Madol World Heritage Site. *Remote Sens.* **2019**, *11*, 2152. [CrossRef]
49. Evans, D.H.; Fletcher, R.J.; Pottier, C.; Chevance, J.-B.; Soutif, D.; Tan, B.S.; Im, S.; Ea, D.; Tin, T.; Kim, S.; et al. Uncovering archaeological landscapes at Angkor using lidar. *Proc. Natl. Acad. Sci. USA* **2013**, *110*, 12595–12600. [CrossRef]
50. Evans, D.; Fletcher, R. The landscape of Angkor Wat redefined. *Antiquity* **2015**, *89*, 1402–1419. [CrossRef]
51. Fernandez-Diaz, J.C.; Carter, W.E.; Shrestha, R.L.; Glennie, C.L. Now You See It . . . Now You Don't: Understanding Airborne Mapping LiDAR Collection and Data Product Generation for Archaeological Research in Mesoamerica. *Remote Sens.* **2014**, *6*, 9951–10001. [CrossRef]
52. Fisher, C.T.; Fernández-Diaz, J.C.; Cohen, A.S.; Cruz, O.N.; Gonzáles, A.M.; Leisz, S.J.; Pezzutti, F.; Shrestha, R.; Carter, W. Identifying Ancient Settlement Patterns through LiDAR in the Mosquitia Region of Honduras. *PLoS ONE* **2016**, *11*, e0159890. [CrossRef]
53. Iriarte, J.; Robinson, M.; De Souza, J.; Damasceno, A.; Da Silva, F.; Nakahara, F.; Ranzi, A.; Aragao, L. Geometry by Design: Contribution of Lidar to the Understanding of Settlement Patterns of the Mound Villages in SW Amazonia. *J. Comput. Appl. Archaeol.* **2020**, *3*, 151–169. [CrossRef]
54. Campana, S. Drones in Archaeology. State-of-the-art and Future Perspectives. *Archaeol. Prospect.* **2017**, *24*, 275–296. [CrossRef]
55. Forte, M.; Campana, S. (Eds.) *Digital Methods and Remote Sensing in Archaeology: Archaeology in the Age of Sensing*; Springer: Cham, Switzerland, 2017.
56. Palka, J.W.; Sánchez Balderas, F.; Hollingshead, I.; Balsanelli, A.; Hernández, C.; Juárez, S.; Lozada Toledo, J.; McGee, R.J.; Salgado-Flores, S. Long-Term Collaborative Research with Lacandon Maya at Mensäbäk, Chiapas, Mexico. In *The Mayanist*; American Foreign Academic Research: Davidson, NC, USA, 2020; Volume 2, pp. 1–20.
57. Davis, D.S.; Buffa, D.; Rasolondrainy, T.; Creswell, E.; Anyanwu, C.; Ibirogba, A.; Randolph, C.; Ouarghidi, A.; Phelps, L.N.; Lahiniriko, F.; et al. The aerial panopticon and the ethics of archaeological remote sensing in sacred cultural spaces. *Archaeol. Prospect.* **2021**, *28*, 305–320. [CrossRef]
58. Golden, C.; Scherer, A.K.; Schroder, W.; Murtha, T.; Morell-Hart, S.; Diaz, J.C.F.; Álvarez, S.D.P.J.; Firpi, O.A.; Agostini, M.; Bazarsky, A.; et al. Airborne Lidar Survey, Density-Based Clustering, and Ancient Maya Settlement in the Upper Usumacinta River Region of Mexico and Guatemala. *Remote Sens.* **2021**, *13*, 4109. [CrossRef]
59. Golden, C.; Scherer, A.K. Territory, Trust, Growth, and Collapse in Classic Period Maya Kingdoms. *Curr. Anthr.* **2013**, *54*, 397–435. [CrossRef]
60. Scherer, A.; Golden, C. *Revisiting Maler's Usumacinta: Recent Archaeological Investigations in Chiapas, Mexico*; Precolumbia Mesoweb Press: San Francisco, CA, USA, 2012.
61. Aliphat Fernández, M.M. Classic Maya Landscape in the Upper Usumacinta River Valley. Ph.D. Dissertation, University of Calgary, Calgary, AB, Canada, 1994.
62. Anaya Hernández, A. *Site Interaction and Political Geography in the Upper Usumacinta Region. during the Late Classic: A GIS Approach*; BAR International Series 994; J. and E. Hedges: Oxford, UK, 2001.
63. Rands, R.L. The Classic Maya collapse: Usumacinta zone and the northwestern periphery. In *The Classic Maya collapse*; Culbert, T.P., Ed.; University of New Mexico Press: Albuquerque, NM, USA, 1973; pp. 165–206.
64. Golden, C.; Scherer, A.K. Border Problems: Recent Archaeological Research along the Usumacinta River. *PARI J.* **2006**, *7*, 1–16.
65. Golden, C.; Scherer, A.K.; Muñoz, A.R.; Vasquez, R. Piedras Negras and Yaxchilan: Divergent Political Trajectories in Adjacent Maya Polities. *Lat. Am. Antiq.* **2008**, *19*, 249–274. [CrossRef]
66. Gorelick, N.; Hancher, M.; Dixon, M.; Ilyushchenko, S.; Thau, D.; Moore, R. Google Earth Engine: Planetary-scale geospatial analysis for everyone. *Remote Sens. Environ.* **2017**, *202*, 18–27. [CrossRef]
67. Louis, J. L2A team Sentinel 2, S2 MPC, Leven-2A Algorithm Theoretical Basis Document. Available online: https://sentinel.esa.int/documents/247904/446933/Sentinel-2-Level-2A-Algorithm-Theoretical-Basis-Document-ATBD.pdf/fe5bacb4-7d4c-9212-8606-6591384390c3?t=1618563205231 (accessed on 26 October 2021).
68. Olofsson, P.; Foody, G.M.; Herold, M.; Stehman, S.V.; Woodcock, C.E.; Wulder, M.A. Good practices for estimating area and assessing accuracy of land change. *Remote Sens. Environ.* **2014**, *148*, 42–57. [CrossRef]
69. Golden, C.; Munkvold, I.; Girardi, S. Estudio preliminar por LiDAR en Piedras Negras. In *Proyecto Paisaje Piedras Negras-Yaxchilán: Informe de la Segunda Temporada de Investigación Presentado ante el Instituto de Antropología e Historia*; Urquizú, M., Scherer, A.K., Golden, C., Eds.; Instituto de Antropología e Historia: Guatemala City, Guatemala, 2017; pp. 157–163.
70. Golden, C.; Murtha, T.; Cook, B.; Shaffer, D.S.; Schroder, W.; Hermitt, E.J.; Firpi, O.A.A.; Scherer, A.K. Reanalyzing environmental lidar data for archaeology: Mesoamerican applications and implications. *J. Archaeol. Sci. Rep.* **2016**, *9*, 293–308. [CrossRef]
71. Murtha, T.; Broadbent, E.N.; Fernández-Diaz, J.C.; Golden, C.; Scherer, A.K. Aplicaciones de sistemas de lidar mediante vehículo aéreo no tripulado y avión. In *Proyecto Arqueológico Busiljá-Chocoljá: Informe de la décima temporada de investigación presentado ante el Consejo de Arqueología del Instituto Nacional de Antropología e Historia*; Scherer, A.K., Golden, C., Eds.; Instituto Nacional de Antropología e Historia: Mexico City, Mexico, 2019; pp. 346–351.
72. Klápště, P.; Fogl, M.; Barták, V.; Gdulová, K.; Urban, R.; Moudrý, V. Sensitivity analysis of parameters and contrasting performance of ground filtering algorithms with UAV photogrammetry-based and LiDAR point clouds. *Int. J. Digit. Earth* **2020**, *13*, 1672–1694. [CrossRef]

73. Kokalj, Ž.; Hesse, R. *Airborne Laser Scanning Raster Data Visualization: A Guide to Good Practice*; Založba ZRC: Ljubljana, Slovenia, 2017.
74. Lozić, E.; Štular, B. Documentation of Archaeology-Specific Workflow for Airborne LiDAR Data Processing. *Geosciences* **2021**, *11*, 26. [CrossRef]
75. Štular, B.; Lozić, E. Comparison of Filters for Archaeology-Specific Ground Extraction from Airborne LiDAR Point Clouds. *Remote Sens.* **2020**, *12*, 3025. [CrossRef]
76. Štular, B.; Eichert, S.; Lozić, E. Airborne LiDAR Point Cloud Processing for Archaeology. Pipeline and QGIS Toolbox. *Remote Sens.* **2021**, *13*, 3225. [CrossRef]
77. Guzmán-López, P. Reconocimiento arqueológico en los alrededores de La Mar. In *Proyecto Arqueológico Busiljá-Chocoljá: Informe de la Cuarta Temporada de Investigación Presentado ante el Consejo de Arqueología del Instituto Nacional de Antropología e Historia*; Scherer, A.K., Golden, C., Dobereiner, J., Eds.; Instituto Nacional de Antropología e Historia: Mexico City, Mexico, 2013; pp. 120–141.
78. Schroder, W. Reconocimiento arqueológico en los ranchos Santa Marta y Tres Piedras, Nueva Esperanza Progresista. In *Proyecto Arqueológico Busiljá-Chocoljá: Informe de la Sexta Temporada de Investigación Presentado ante el Consejo de Arqueología del Instituto Nacional de Antropología e Historia*; Schroder, W., Golden, C., Scherer, A.K., Eds.; Instituto Nacional de Antropología e Historia: Mexico City, Mexico, 2015; pp. 99–110.
79. Schroder, W. Reconocimiento en Arroyo Belén, La Selva, Busiljá, Nuevo Guerrero, Nuevo Jerusalén, Nuevo Pedregal, y Ojo de Agua Zapote. In *Proyecto Arqueológico Busiljá-Chocoljá: Informe de la Novena Temporada de Investigación Presentado ante el Consejo de Arqueología del Instituto Nacional de Antropología e Historia*; Scherer, A.K., Golden, C., Eds.; Instituto Nacional de Antropología e Historia: Mexico City, Mexico, 2018; pp. 200–220.
80. del Pilar, S.J.A.; Sobrino Fernández, S.A.; Ojeda González, S.; Borges Barrientos, J.L. Descripciones de las cerámicas procedentes de los sitios arqueológicos Lacanjá Tzeltal, Rancho Poniente, y Sacrificios, Chiapas. In *Proyecto Arqueológico Busiljá-Chocoljá: Informe de la Novena Temporada de Investigación Presentado ante el Consejo de Arqueología e Historia*; Scherer, A.K., Golden, C., Eds.; Instituto Nacional de Antropología e Historia: Mexico City, Mexico, 2018; pp. 300–311.
81. del Pilar, S.J.A.; Sobrino Fernández, S.A.; Ojeda González, S.; Borges Barrientos, J.L. Tipología de las cerámicas de los sitios arqueológicos Lacanjá Tzeltal, Rancho Poniente y Sacrificios, Chiapas. In *Proyecto Arqueológico Busiljá-Chocoljá: Informe de la Novena Temporada de Investigación Presentado ante el Consejo de Arqueología del Instituto Nacional de Antropología e Historia*; Scherer, A.K., Golden, C., Eds.; Instituto Nacional de Antropología e Historia: Mexico City, Mexico, 2018; pp. 312–345.
82. Ramiro Talavera, M.Y.; Ojeda González, S.; Schnell, J. Las Limas: Investigaciones preliminares. In *Proyecto Arqueológico Busiljá-Chocoljá: Informe de la Décima Temporada de Investigación Presentado ante el Consejo de Arqueología del Instituto Nacional de Antropología e Historia*; Scherer, A.K., Golden, C., Eds.; Instituto Nacional de Antropología e Historia: Mexico City, Mexico, 2019; pp. 302–321.
83. Seidita, M.; Ojeda González, S.; Kollias, G.V., III; Talavera, M. Reconocimiento en Ricardo Flores Magón y el Ejido de Sacrificio. In *Proyecto Arqueológico Busiljá-Chocoljá: Informe de la Novena Temporada de Investigación Presentado ante el Consejo de Arqueología del Instituto Nacional de Antropología e Historia*; Scherer, A.K., Golden, C., Eds.; Instituto Nacional de Antropología e Historia: Mexico City, Mexico, 2018; pp. 110–152.
84. Alcover Firpi, O. Conflict, Defense, and Cooperation at Macabilero, Peten, Guatemala. Ph.D. Dissertation, Brown University, Providence, RI, USA, 2020.
85. Schroder, W. Community Resilience through Crisis at El Infiernito, Chiapas, a Fortified Refuge in the Upper Usumacinta Valley. Ph.D. Dissertation, University of Pennsylvania, Philadelphia, PA, USA, 2019.
86. Schroder, W. Cycles of defence on the Piedras Negras kingdom periphery: Landscape patrimony at the fortified hilltop community of El Infiernito, Chiapas. *Landsc. Res.* **2021**, *46*, 793–810. [CrossRef]
87. Davenport, B.; Guzmán-López, P.; Delgado Arévalo, J.H. Vallescondido: Investigaciones preliminares. In *Proyecto Arqueológico Busiljá-Chocoljá: Informe de la Tercera Temporada de Campo Presentado ante el Consejo de Arqueología del Instituto Nacional de Antropología e Historia*; Scherer, A.K., Golden, C., Dobereiner, J., Eds.; Instituto Nacional de Antropología e Historia: Mexico City, Mexico, 2012; pp. 167–169.
88. Golden, C.; Morell-Hart, S.; Murtha, T.; Scherer, A.K.; Broadbent, E.N.; Schroder, W.; Bérubé, É.; Dine, H. Campos canalizados en el Ejido de Nuevo Canán, Palenque. In *Proyecto Arqueológico Busiljá-Chocoljá: Informe de la Décima Temporada de Investigación Presentado ante el Consejo de Arqueología del Instituto Nacional de Antropología e Historia*; Scherer, A.K., Golden, C., Eds.; Instituto Nacional de Antropología e Historia: Mexico City, Mexico, 2019; pp. 341–345.
89. Golden, C.; Scherer, A.K. Rancho El Edén, Nuevo Guerrero y Nuevo Francisco León. In *Proyecto Arqueológico Busiljá-Chocoljá: Informe de la Segunda Temporada de Investigación Presentado ante el Consejo de Arqueología del Instituto Nacional de Antropología e Historia*; Golden, C., Scherer, A.K., Eds.; Instituto Nacional de Antropología e Historia: Mexico City, Mexico, 2011; pp. 71–77.
90. Schroder, W. Reconocimiento arqueológico en los alrededores de Nuevo Guerrero, Ocosingo. In *Proyecto Arqueológico Busiljá-Chocoljá: Informe de la Sexta Temporada de Investigación Presentado ante el Consejo de Arqueología del Instituto Nacional de Antropología e Historia*; Schroder, W., Golden, C., Scherer, A.K., Eds.; Instituto Nacional de Antropología e Historia: Mexico City, Mexico, 2015; pp. 111–121.
91. Schroder, W.; Golden, C.W.; Scherer, A.K.; Jiménez Álvarez, S.; Del, P.; Dobereiner, J.; Méndez Cab, A. At the Crossroads of Kingdoms: Recent Investigations on the Periphery of Piedras Negras and Its Neighbors. *PARI J.* **2017**, *17*, 1–15.

92. Schroder, W. Reconocimiento arqueológico en Nuevo Francisco León y Nuevo Guerrero, Ocosingo. In *Proyecto Arqueológico Busiljá-Chocoljá: Informe de la Séptima Temporada de Investigación Presentado ante el Consejo de Arqueología del Instituto Nacional de Antropología e Historia*; Schroder, W., Golden, C., Scherer, A.K., Eds.; Instituto Nacional de Antropología e Historia: Mexico City, Mexico, 2016; pp. 110–127.
93. Scherer, A.K.; Golden, C. Water in the west: Chronology and collapse of the Western Maya river kingdoms. In *The Great Maya Droughts in Cultural Context*; Iannone, G., Ed.; University Press of Colorado: Boulder, CO, USA, 2014; pp. 207–229.
94. Dine, H.; Ramiro Talavera, M.Y.; Bérubé, É.; Scherer, A. El Pozo de Nuevo Tumbalá: Investigaciones preliminares. In *Proyecto Arqueológico Busiljá-Chocoljá: Informe de la Décima Temporada de Investigación Presentado ante el Consejo de Arqueología del Instituto Nacional de Antropología e Historia*; Scherer, A.K., Golden, C., Eds.; Instituto Nacional de Antropología e Historia: Mexico City, Mexic, 2019; pp. 260–301.
95. Anaya Hernández, A.; Guenter, S.; Zender, M. Sak Tz'i', a Classic Maya Center: A Locational Model Based on GIS, and Epigraphy. *Lat. Am. Antiq.* **2003**, *14*, 179–191. [CrossRef]
96. Bíró, P. Sak Tz'i' in the Classic Period Hieroglyphic Inscriptions. Available online: www.mesoweb.com/articles/biro/SakTzi.html (accessed on 18 November 2021).
97. Golden, C.; Scherer, A.K.; Houston, S.; Schroder, W.; Morell-Hart, S.; del Pilar, S.J.A.; Kollias, G.V.; Ramiro Talavera, M.Y.; Matsumoto, M.; Dobereiner, J.; et al. Centering the Classic Maya Kingdom of Sak Tz'i'. *J. Field Archaeol.* **2020**, *45*, 67–85. [CrossRef]
98. Matsumoto, M.E.; Scherer, A.K.; Golden, C.; Houston, S. Sculptural Traditionalism and Innovation in the Classic Maya Kingdom of Sak Tz'i', Mexico. *Anc. Mesoam.* **2021**, 1–24. [CrossRef]
99. Flores Esquivel, A. Levantamiento topográfico y arquitectónico en Lacanjá Tzeltal. In *Proyecto Arqueológico Busiljá-Chocoljá: Informe de la Décima Temporada de Investigación Presentado ante el Consejo de Arqueología del Instituto Nacional de Antropología e Historia*; Scherer, A.K., Golden, C., Eds.; Instituto Nacional de Antropología e Historia: Mexico City, Mexico, 2019; pp. 15–35.
100. Golden, C.; Scherer, A. Lacanjá Tzeltal: Descripción y mapa del sitio. In *Proyecto Arqueológico Busiljá-Chocoljá: Informe de la Novena Temporada de Investigación Presentado ante el Consejo de Arqueología del Instituto Nacional de Antropología e Historia*; Scherer, A.K., Golden, C., Eds.; Instituto Nacional de Antropología e Historia: Mexico City, Mexico, 2018; pp. 153–167.
101. Ramiro Talavera, M.Y.; Kollias, G.V., III. Lacanjá Tzeltal: Excavaciones preliminares. In *Proyecto Arqueológico Busiljá-Chocoljá: Informe de la Novena Temporada de Investigación Presentado ante el Consejo de Arqueología del Instituto Nacional de Antropología e Historia*; Scherer, A.K., Golden, C., Eds.; Instituto Nacional de Antropología e Historia: Mexico City, Mexico, 2018; pp. 168–199.
102. Mayer, K.H. The Maya Ruins of Primera Sección, Chiapas, Mexico. *Mexicon* **2006**, *28*, 63–66.
103. Schroder, W. Reconocimiento en Benemérito de las Américas, Primera Sección. In *Proyecto Arqueológico Busiljá-Chocoljá: Informe de la Octava Temporada Presentado ante el Consejo de Arqueología*; Schroder, W., Golden, C., Scherer, A.K., Eds.; Instituto Nacional de Antropología e Historia: Mexico City, Mexico, 2017; pp. 171–180.
104. Tovalín, A.; Ortiz, V. El Sitio Arqueológico de La Primera Sección de Benemérito de Las Américas, Chiapas. *Arqueología* **2005**, *35*, 33–49.
105. Mejía-Ramón, A. La prospección fotogramétrica fluvial y aérea. In *Informe del Proyecto Geomorfológico de Asentamientos Antiguos del Usumacinta Superior, la Temporada de 2019: Investigando la Historia Fluvial y los Patrones de Asentamiento de Altar de Sacrificios y sus Alrededores*; Munson, J., Paiz Aragón, L., Eds.; Instituto Nacional de Antropología e Historia: Mexico City, Mexico, 2019; pp. 12–35.
106. Schroder, W. Benemérito de las Américas, Primera Sección: Investigaciones preliminares. In *Proyecto Arqueológico Busiljá-Chocoljá: Informe de la Décima Temporada Presentado ante el Consejo de Arqueología*; Scherer, A.K., Golden, C., Eds.; Instituto Nacional de Antropología e Historia: Mexico City, Mexico, 2019.
107. Cook, B.; Corp, L.; Nelson, R.; Middleton, E.; Morton, D.; McCorkel, J.; Masek, J.; Ranson, K.; Ly, V.; Montesano, P. NASA Goddard's LIDAR, Hyperspectral and Thermal (G-LiHT) Airborne Imager. *Remote Sens.* **2013**, *5*, 4045–4066. [CrossRef]
108. Chen, C.; Guo, J.; Wu, H.; Li, Y.; Shi, B. Performance Comparison of Filtering Algorithms for High-Density Airborne LiDAR Point Clouds over Complex LandScapes. *Remote Sens.* **2021**, *13*, 2663. [CrossRef]
109. Zhao, X.; Su, Y.; Li, W.; Hu, T.; Liu, J.; Guo, Q. A Comparison of LiDAR Filtering Algorithms in Vegetated Mountain Areas. *Can. J. Remote Sens.* **2018**, *44*, 287–298. [CrossRef]
110. Minár, J.; Evans, I.S.; Jenčo, M. A comprehensive system of definitions of land surface (topographic) curvatures, with implications for their application in geoscience modelling and prediction. *Earth-Sci. Rev.* **2020**, *211*, 103414. [CrossRef]